NASA MEMO 3-8-59L

NASA

MEMORANDUM

WIND-TUNNEL INVESTIGATION OF A SMALL-SCALE SWEPTBACK-WING JET-TRANSPORT MODEL EQUIPPED WITH AN EXTERNAL-FLOW JET-AUGMENTED DOUBLE SLOTTED FLAP

By Joseph L. Johnson, Jr.

Langley Research Center
Langley Field, Va.

NATIONAL AERONAUTICS AND SPACE ADMINISTRATION
WASHINGTON
April 1959

NATIONAL AERONAUTICS AND SPACE ADMINISTRATION

MEMORANDUM 3-8-59L

WIND-TUNNEL INVESTIGATION OF A SMALL-SCALE SWEPTBACK-WING JET-TRANSPORT MODEL EQUIPPED WITH AN EXTERNAL-FLOW JET-AUGMENTED DOUBLE SLOTTED FLAP

By Joseph L. Johnson, Jr.

SUMMARY

A wind-tunnel investigation at low speeds has been made to study the aerodynamic characteristics of a small-scale sweptback-wing jet-transport model equipped with an external-flow jet-augmented double slotted flap. Included in the investigation were tests of the wing alone to study the effects of varying the spanwise extent of blowing on the full-span flap.

The results indicated that the double-slotted-flap arrangement of the present investigation was more efficient in terms of lift and drag than were the external-flow single-slotted-flap arrangements previously tested and gave a substantial reduction in the thrust-weight ratio required for a given lift coefficient under trimmed drag conditions. An increase in the spanwise extent of blowing on the full-span flap was also found to increase the efficiency of the model in terms of the lift and drag but, as would be expected on a sweptback-wing configuration, was accompanied by significant increases in negative pitching moment.

INTRODUCTION

In other studies of the jet-augmented flap conducted by the National Aeronautics and Space Administration, the external-flow-type jet-augmented flap was found to be less efficient than the internal-flow type but produced values of jet-circulation lift large enough to warrant consideration for use on airplanes with pod-mounted engines. Since that time, several investigations of external-flow jet-augmented-flap arrangements have been made, in which a study of the dynamic stability and control characteristics of a jet-transport model at very high lift coefficients has been included. (See refs. 1 to 4.)

In the jet-augmented-flap arrangements used in most of these investigations, the jet exhaust from pod-mounted engines was directed

by flat-plate deflectors toward the base of a slotted flap which then directed the jet downward in the form of a flattened jet sheet. Static calibration tests of such a flap arrangement on the jet-transport model of reference 4 indicated that this method of spreading and deflecting the jet exhaust caused fairly large losses in engine thrust. In an effort to reduce these losses, three basic changes were made to the flap arrangement. First, the flat-plate deflectors were replaced by flat nozzles which accomplished the spreading and deflection of the jet exhaust much more efficiently. These flat nozzles were mounted to the engine tail pipes and tilted up toward the base of the slotted flap. Next, the original single slotted flap was replaced by a double slotted flap in which the first flap segment was a thin vane. And finally, the contour of the bottom surface of the wing was altered to permit almost all of the jet to pass through the slot gap between the wing and first flap segment without impinging on the bottom surface of the wing or the face of the flap. The present investigation was made to study the aerodynamic characteristics of the model of reference 4 equipped with this revised jet-augmented-flap arrangement.

The investigation consisted of force tests of the complete model and also of the wing alone for an angle-of-attack range from -8° to 12° and for momentum coefficients up to about 3.0. In addition, tests were made of the wing alone with several combinations of pod-mounted engines located along the wing to study the effects of varying the spanwise extent of blowing on the full-span flap. All tests in the investigation were made at a Reynolds number of about 260,000 based on the mean aerodynamic chord of the wing.

SYMBOLS

The data are referred to the stability system of axes originating at a center of gravity located at 0.40 mean aerodynamic chord and on the fuselage reference line.

C_D drag coefficient, $\frac{\text{Drag}}{qS}$

C_L lift coefficient, $\frac{\text{Lift}}{qS}$

$(C_L)_{C_\mu=0}$ lift coefficient at zero momentum coefficient

$C_{L_\alpha} = \frac{\partial C_L}{\partial \alpha}$ per degree

$C_{L,\Gamma}$ jet-circulation lift coefficient, lift induced by jet sheet

C_m pitching-moment coefficient, $\frac{M_Y}{qS\bar{c}}$

C_μ momentum coefficient based on thrust measured at nozzle, T/qS

c wing chord, ft

$\bar{c}$ mean aerodynamic chord, ft

i_t angle of incidence of horizontal tail, deg

M_Y pitching moment, ft-lb

q dynamic pressure, $\frac{1}{2}\rho V^2$, lb/sq ft

S wing area, sq ft

T thrust at nozzles, lb

V velocity, ft/sec

W weight, lb

α angle of attack, deg

δ_e elevator-deflection angle, deg

δ_{f1} deflection angle of first flap segment, measured with respect to wing reference line and in plane perpendicular to flap hinge line, deg

δ_{f2} deflection angle of second flap segment, measured with respect to first flap segment and in plane perpendicular to flap hinge line, deg

δ_j jet-deflection angle, measured with respect to wing reference line and in a plane perpendicular to flap hinge line, deg

η jet turning and spreading efficiency factor, determined by ratio of thrust of jet reaction at flap to thrust at exhaust nozzle

ρ air density, slugs/cu ft

Pod-location designations:

L_1	left inboard, 0.3 semispan
L_2	left middle, 0.55 semispan
L_3	left outboard, 0.80 semispan
C	center, midspan
R_1	right inboard, 0.3 semispan
R_2	right middle, 0.55 semispan
R_3	right outboard, 0.80 semispan

APPARATUS AND MODEL

The investigation was conducted in the Langley free-flight tunnel. All tests were made with a vertical-strut support system and strain-gage balances.

The sweptback-wing jet-transport model used in the present investigation was the same model used in the investigation of reference 4 except that the original, partial-span, jet-augmented single slotted flap was replaced by a full-span, jet-augmented double slotted flap, and flat nozzles were mounted to the engine tail pipes instead of the flat-plate deflectors to accomplish the spreading and deflection of the jet exhaust. Drawings of the complete model and of the wing alone are presented in figures 1 and 2. Table I gives the dimensional and mass characteristics of the model. The wing of the model had 30° sweep of the quarter-chord, an aspect ratio of 6.60, and a taper ratio of 0.367. The all-movable horizontal tail of the model was located about midspan of the vertical tail, had an area that was 25 percent of the wing area, and was equipped with an inverted slotted flap which served as an elevator. (See fig. 1.)

Pod-mounted engines were simulated on the model by two main nacelles permanently mounted to the wing on pylons and by several simple flat nozzles which were temporarily mounted along the wing at various spanwise stations by removable pylons. The two main nacelles were supplied with compressed air through flexible hoses which passed internally through the model. Compressed air was supplied to each of the removable nacelles through flexible hoses which were attached externally. These

pod-mounted-engine arrangements are illustrated in figure 2 and dimensional characteristics of the flat nozzles tested are given in figure 3(a).

The jet-augmented-flap arrangement used on the model is illustrated in figure 3(a) and dimensional characteristics are given in figure 3(b). The basic geometry of this double-slotted-flap configuration was determined from reference 5 but the wing and flap assembly were modified for the present investigation. For take-off and landing, the jet exhaust is flattened out and directed toward the base of the double slotted flap by flat nozzles which are attached to the engine tail pipes and tilted upward. The double slotted flap then deflects the jet exhaust downward in the form of a jet sheet. The hinge lines and deflection angles of the two flap segments are adjustable so that each segment can be moved independently to obtain the desired slot gap or deflection angle. In order to permit almost all of the jet exhaust to pass through the slot gap between the wing and first flap segment without impinging on the bottom surface of the wing or face of the flap, the contour of the bottom surface of the wing was altered as shown in figure 3(b). The first flap segment was replaced by a thin metal vane in an effort to reduce the thrust loss due to the drag of the flap. For cruising flight, the flap is retracted and the flat nozzles are returned to a horizontal attitude. Data obtained from flat-nozzle design studies at the Langley Research Center and results of reference 6 have shown that properly designed flat nozzles are only slightly less efficient in terms of engine thrust than are circular nozzles. In the cruising condition, some means of providing a smooth fairing over that portion of the bottom surface of the wing and flap assembly which was altered for the landing condition would be required. No attempt was made to provide such a fairing in these tests, however, since the present investigation was concerned primarily with the landing condition.

TESTS

Force tests were made to determine the aerodynamic characteristics of the model over an angle-of-attack range from -8° to 12° for several flap deflections and for momentum coefficients up to about 3.0. These tests were made with two-pod and four-pod arrangements. In addition, tests were made of the wing alone at 0° angle of attack for several pod-mounted-engine arrangements to study the effects on the lift, drag, and pitching-moment characteristics of varying the spanwise extent of blowing on the full-span flap.

All the tests in this investigation were made at a dynamic pressure of about 1.65 pounds per square foot which corresponds to a velocity of about 37 feet per second and to a Reynolds number of about 260,000 based on the mean aerodynamic chord of the wing.

REDUCTION OF DATA

No wind-tunnel corrections have been applied to the data and no corrections were applied for the effects of the model support and of the flexible air hoses. The main purpose of these tests was to determine the forces and moments acting on the model at low scale to supplement free-flight investigations of the same model under similar test conditions. Although these data are thought to indicate qualitatively the effects of the major modifications to the flap and blowing arrangements, they are not sufficiently accurate to allow numerical comparison.

The momentum coefficient C_μ presented in this report is defined as T/qS where T is the measured thrust of the flat nozzles as determined from calibration tests. This coefficient C_μ is approximately equivalent to the momentum coefficient which has been used in boundary-layer-control investigations and in the jet-augmented-flap investigations, such as that reported in reference 7. In order to determine thrust losses in spreading and deflecting the jet, values of thrust were obtained from force measurements made during static calibrations of the cruising condition (flaps retracted and flat nozzles in horizontal attitude) and of the landing condition (flaps extended and flat nozzles tilted upward). Comparison of the calibration data for these two conditions indicated that the losses caused by spreading and deflecting the jets varied from about 10 or 15 percent for a jet-deflection angle of 40° to about 20 percent for a jet-deflection angle of 65°.

RESULTS AND DISCUSSION

Calibration of Jet-Deflection Angles

A plot of the average jet-deflection angles produced by given flap settings is presented in figure 4. These data show that a combined flap setting of 30° produced a jet-deflection angle of about 40° and that combined flap settings of 60° and 70° produced jet-deflection angles of about 55° and 65°, respectively. Actually, the jet-deflection angle should have been greater than the corresponding flap setting in all cases since the geometric flap angle is referred to the reference line of the wing, whereas the jet-deflection angle is determined by the upper surface angle of the flap. For this particular flap arrangement, however, the contour of the upper surface of the flap at the higher flap settings was apparently too great for the jet exhaust to follow. For a given flap setting, the four-pod arrangement gave consistently lower jet-deflection angles than did the two-pod arrangement.

Complete Model

The results of the tests to determine the aerodynamic characteristics of the complete model for the two-pod and four-pod arrangements are presented in figures 5 to 10 and are summarized in figures 11 to 14. The data are presented for jet-deflection angles of 36° to 67°.

Lift characteristics.- The basic data of figures 5 to 10 show an increase in lift coefficient and, in general, an increase in lift-curve slope with increasing C_μ which is characteristic of configurations equipped with jet-augmented flaps. The four-pod configuration generally produced higher lift coefficients for given values of C_μ than did the two-pod configuration. For a better comparison of the lift characteristics at a given value of C_μ, the data for the tail-off configurations are replotted for 0° angle of attack in figures 11(a) and 11(b). The data of these figures show the increase in lift coefficient with increasing flap deflection and the gain in lift in changing from the two-pod to the four-pod configuration.

In order to compare the lifting capabilities of the external-flow jet-augmented single- and double-slotted-flap arrangements, the lift data from figure 11(a) of the present report and from figure 13 of reference 3 were examined in terms of the expression

$$C_{L,\Gamma} = C_L - (C_L)_{C_\mu=0} - \eta C_\mu \sin(\alpha + \delta_j)$$

For simplicity, the two flap arrangements are referred to in the discussion of these data as jet-augmented single and double slotted flaps. Actually, as pointed out in the sections entitled "Introduction" and "Apparatus and Model," there are several differences in the geometry of the single- and double-slotted-flap arrangements. All of these differences should be considered when comparisons between the aerodynamic characteristics of these two flap arrangements are made.

The various components which make up the total lift coefficient were determined for a jet-deflection angle of 57° and are presented in figure 12. The data of figure 12 show that the single- and double-slotted-flap arrangements were about equally effective in producing jet-circulation lift but the double-slotted-flap arrangement produced higher values of total lift coefficient because of larger increments of lift at zero momentum coefficient.

Pitching-moment characteristics.- The data of figures 5 to 10 show that, for the tail-off configurations, the negative pitching moments increased and the static instability generally decreased with increasing C_μ. These variations in pitching-moment characteristics are similar to

those shown in previous investigations on jet-augmented flaps. The data of figures 11(a) and 11(b) show that these negative pitching moments increased with increasing flap deflection and that the gain in lift coefficient obtained by changing from the two-pod to the four-pod arrangement was accompanied by an increase in negative pitching moment. In order to obtain a better indication of some of the fundamental reasons for these variations in pitching-moment characteristics for unstalled conditions near $\alpha = 0^{\circ}$, the data of figures 6(a) and 9(a) were used to obtain lift-curve slope, center of pressure, and aerodynamic center for the tail-off configurations at several values of C_{μ}. These data are presented in figure 13 together with similar results for the jet-augmented single-slotted-flap arrangement of reference 3. The jet-deflection angles varied from 54° to 60° but this difference in jet-deflection angle is believed to have only a small effect on the results presented in figure 13.

The data of the upper portion of figure 13 show that, although the lift-curve slope of the double slotted flap was greater than that for the single slotted flap at $C_{\mu} = 0$, the rate of increase in $C_{L_{\alpha}}$ with C_{μ} was generally about the same in either case for the two-pod configuration. The rate of increase in lift-curve slope with C_{μ} for the four-pod configuration was greater than those for the other configurations. This increase in $C_{L_{\alpha}}$ with increasing C_{μ} accounts partly for the decrease in instability with increasing C_{μ} for the tail-off configurations.

The data of the lower portion of figure 13 show that at the lower values of C_{μ} the center of pressure for the double-slotted-flap configuration was located about 10 percent mean aerodynamic chord rearward of that for the single slotted flap. An interesting point brought out by the data of figure 13 is that, although the center of pressure was more rearward for the double-slotted-flap configuration, the aerodynamic center for this arrangement was also more rearward than that for the single slotted flap with the net result that the distance from the flap center of pressure to the aerodynamic center in either case was not greatly different. This result suggests the possibility that the center-of-gravity position for the double-slotted-flap arrangement could be moved rearward to reduce the large negative pitching moment inherent in this type of flap arrangement if this rearward center-of-gravity position did not lead to unsatisfactory stability for the cruise condition.

From an analysis of the tail-on data of figures 5 to 10 it appears that, with the center of gravity located at 40 percent mean aerodynamic chord, the relatively large horizontal tail used in the present investigation provided stability at negative and small positive angles of attack but was inadequate for trimming at lift coefficients higher than 2 or 3.

Drag characteristics.- The drag characteristics of the model of the present investigation (figs. 5 to 10) were examined in terms of the thrust-weight ratio T/W required to achieve a given lift coefficient at trimmed drag ($C_D = 0$) conditions. An examination of the data in this manner takes into consideration the thrust recovery as well as the lift characteristics of the model and gives an approximate indication of the overall effectiveness of a given jet-augmented-flap arrangement for steady, level-flight conditions. For purposes of comparison, a similar analysis of the data of the jet-augmented single-slotted-flap arrangement of reference 3 was made.

The results of this analysis are presented in figure 14 for the double-slotted-flap model in the two-pod and four-pod arrangements and for the single-slotted-flap model of reference 3 in a two-pod arrangement. The data of this figure show that for a given lift coefficient the double-slotted-flap model in the four-pod arrangement could be trimmed in drag for a lower value of T/W than could the two-pod arrangement, particularly at the higher jet-deflection angles. At a lift coefficient of about 5.5 (the only test point available for comparison of the two flap arrangements) the single-slotted-flap arrangement was considerably less efficient in terms of T/W required for trimmed drag than were the double-slotted-flap arrangements.

Wing Alone

The data obtained from tests to study the effects on the aerodynamic characteristics of the wing alone of varying the extent of spanwise blowing on the full-span flap are presented in figure 15. These tests were made at 0° angle of attack and for a geometric flap angle of 60°.

The data of figure 15 generally show an increase in lift coefficient for a given C_μ as the spanwise extent of blowing on the full-span flap was increased from the center pod arrangement C, which covered about 15 percent of the wing span, to the seven-pod arrangement $L_3L_2L_1CR_1R_2R_3$, which covered about 95 percent of the wing span.

From the lift data of figure 15, values of jet-circulation lift coefficient were determined for the various combinations of pod arrangements investigated. These values of $C_{L,\Gamma}$ are presented as a function of C_μ in figure 16 and show that increasing the spanwise extent of blowing on the full-span flap produced an increase in $C_{L,\Gamma}$ for a given value of C_μ. An analysis of the lift data of figure 16 indicates that

blowing near the center portion of the wing (pod positions C and L_1CR_1) produced values of jet-circulation lift which were greater than the values of $C_{L,\Gamma}$ that would be expected from full-span blowing over low-aspect-ratio wings having spans corresponding to the portions of the wing covered by the jet exhaust for these two pod arrangements. These relatively high values of $C_{L,\Gamma}$ produced by blowing over the center portion of the full-span flap apparently result from some spanwise flow down the flap brought about by sweep of the wing and also from some carryover of the jet-circulation lift distribution to the wing outboard of the jet exhaust.

The data of figure 15 show that the increase in lift coefficient that is realized from an increase in the spanwise extent of blowing on the full-span flap is also accompanied by an increase in negative pitching moment. This increase in negative pitching moment results from the fact that, as the spanwise extent of blowing is increased, the jet exhaust covers portions of the swept wing which are farther outboard and, therefore, farther rearward of the center of gravity.

The effect on the drag characteristics of the wing alone of varying the spanwise extent of blowing on the full-span flap was studied in terms of the thrust-weight ratio required for trimmed drag. These data, presented in figure 17, show that the thrust-weight ratio required for these conditions was reduced somewhat by an increase in the spanwise extent of blowing. It should be pointed out that, although these data are believed to indicate qualitatively the effect of varying the spanwise extent of blowing on the full-span flap, the values of T/W plotted in figure 17 are not directly comparable with the data for the wing-fuselage combination of figure 14 since no corrections were applied to the basic data to account for the relatively large effects of the flexible hoses on the drag characteristics of the wing-alone configuration.

SUMMARY OF RESULTS

The results of the wind-tunnel investigation at low speeds to study the aerodynamic characteristics of a sweptback-wing jet-transport model equipped with an external-flow jet-augmented double slotted flap may be summarized as follows:

1. The double-slotted-flap arrangement of the present investigation was found to be more efficient in terms of lift and drag than were external-flow single-slotted-flap arrangements previously tested and gave a substantial reduction in the thrust-weight ratio required for a given lift coefficient under trimmed drag conditions.

2. An increase in the spanwise extent of blowing on the full-span flap was also found to increase the efficiency of the model in terms of the lift and drag but, as would be expected on a sweptback-wing configuration, was accompanied by significant increases in negative pitching moment.

Langley Research Center,
National Aeronautics and Space Administration,
Langley Field, Va., December 22, 1958.

REFERENCES

1. Campbell, John P., and Johnson, Joseph L., Jr.: Wind-Tunnel Investigation of an External-Flow Jet-Augmented Slotted Flap Suitable for Application to Airplanes With Pod-Mounted Jet Engines. NACA TN 3898, 1956.

2. Davenport, Edwin E.: Wind-Tunnel Investigation of External-Flow Jet-Augmented Double Slotted Flaps on a Rectangular Wing at an Angle of Attack of 0° to High Momentum Coefficients. NACA TN 4079, 1957.

3. Johnson, Joseph L., Jr.: Wind-Tunnel Investigation of the Static Longitudinal Stability and Trim Characteristics of a Sweptback-Wing Jet-Transport Model Equipped With an External-Flow Jet-Augmented Flap. NACA TN 4177, 1958.

4. Johnson, Joseph L., Jr.: Wind-Tunnel Investigation at Low Speeds of Flight Characteristics of a Sweptback-Wing Jet-Transport Airplane Model Equipped With an External-Flow Jet-Augmented Slotted Flap. NACA TN 4255, 1958.

5. Harris, Thomas A., and Recant, Isidore G.: Wind-Tunnel Investigation of NACA 23012, 23021, and 23030 Airfoils Equipped With 40-Percent-Chord Double Slotted Flaps. NACA Rep. 723, 1941.

6. Coles, Willard D., and Callaghan, Edmund E.: Full-Scale Investigation of Several Jet-Engine Noise-Reduction Nozzles. NACA TN 3974, 1957.

7. Lockwood, Vernard E., Turner, Thomas R., and Riebe, John M.: Wind-Tunnel Investigation of Jet-Augmented Flaps on a Rectangular Wing to High Momentum Coefficients. NACA TN 3865, 1956.

TABLE I

DIMENSIONAL AND MASS CHARACTERISTICS OF THE MODEL

Wing:	
Area, sq ft	6.95
Aspect ratio	6.60
$\bar{c}$, ft	1.10
Airfoil section, root	NACA 65_1-412
Airfoil section, tip	NACA 65_1-412
Flap chord, percent wing chord	30.0
Flap span, percent wing span	100.0
Root chord, ft	1.5
Tip chord, ft	0.55
Span, ft	6.75
Taper ratio	0.367
Sweep of quarter-chord, deg	30
Horizontal tail:	
Area (total), sq ft	1.74
Length (distance from 0.40$\bar{c}$ of wing to 0.25$\bar{c}$ of tail), chords	2.94
Span ft	2.87
Root chord, ft	0.96
Tip chord, ft	0.31
$\bar{c}$, ft	0.69
Aspect ratio	4.84
Sweep of leading edge, deg	38
Taper ratio	0.32
Airfoil section	NACA 65-009
Vertical tail:	
Exposed area, sq ft	1.31
Exposed span, ft	1.45
Root chord at fuselage intersection, ft	1.17
Tip chord, ft	0.63
Sweep of leading edge, deg	30
Airfoil section	NACA 65-009

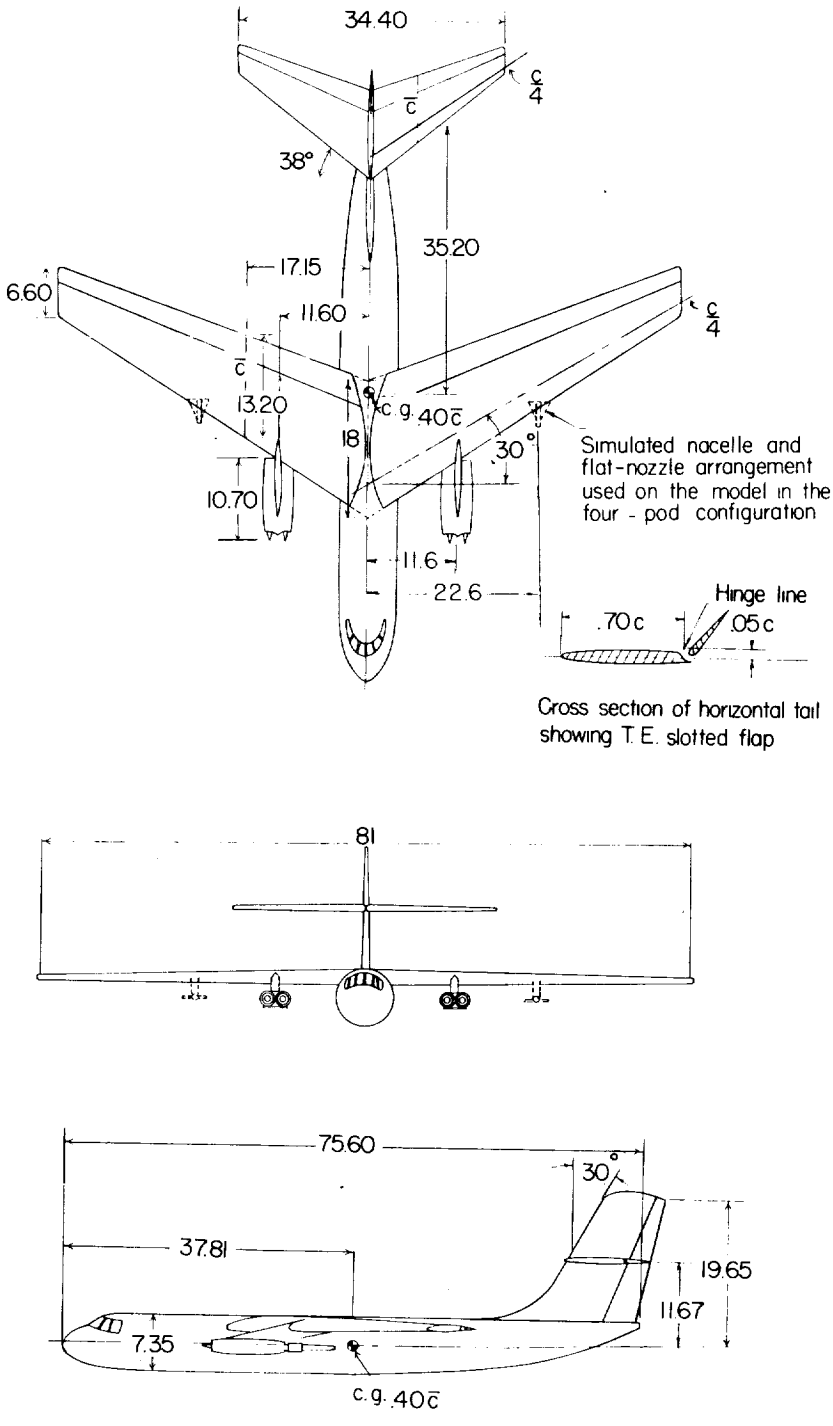

Figure 1.- Three-view drawing of sweptback-wing jet-transport model used in the investigation. All dimensions are in inches.

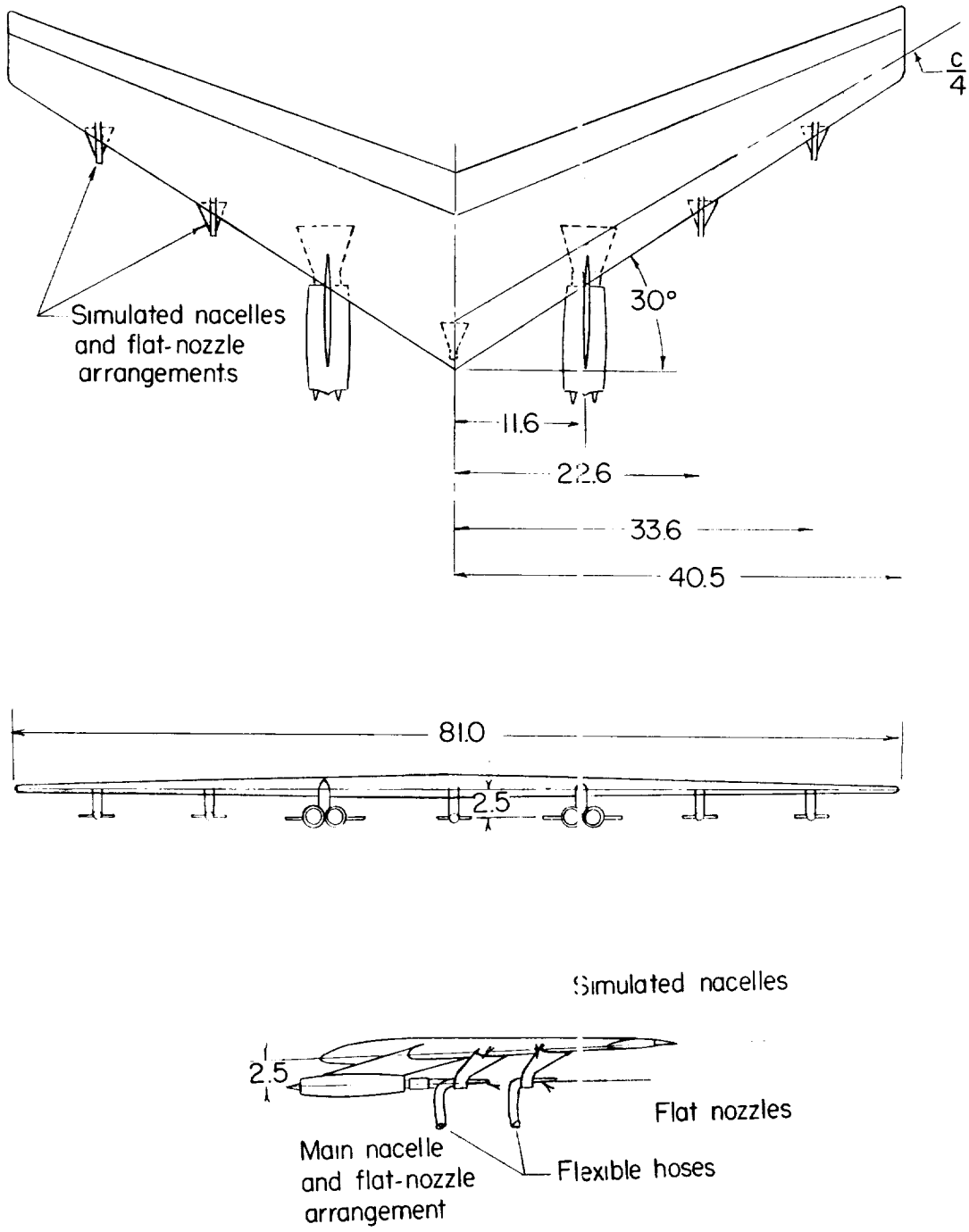

Figure 2.- Sweptback wing with main nacelles and simulated nacelles equipped with flat nozzles. All dimensions are in inches.

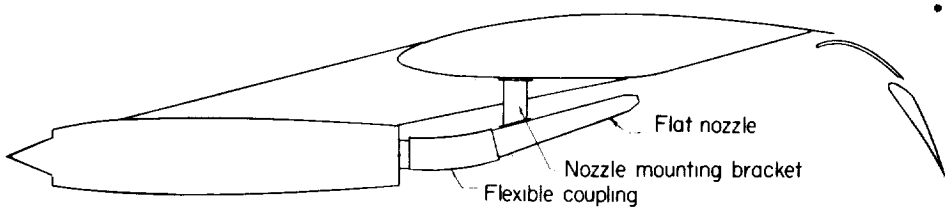

Cross section of wing for landing condition

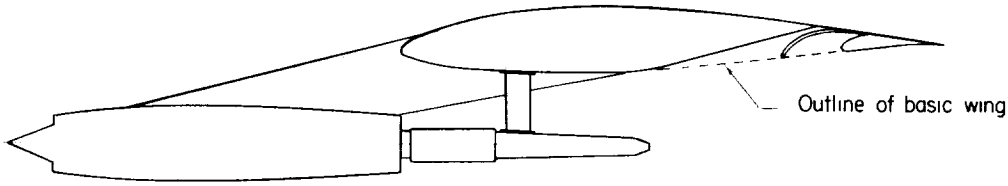

Cross section of wing for cruising flight condition

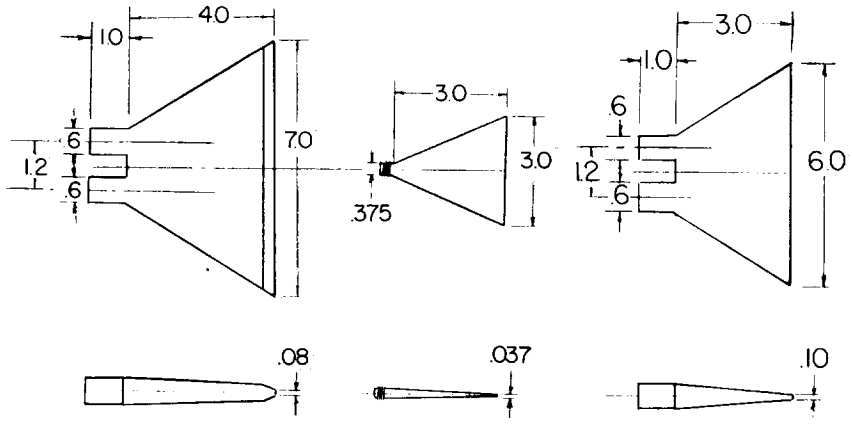

(a) Double slotted flap and flat nozzles.

Figure 3.- Arrangement of external-flow jet-augmented double slotted flap and flat nozzles used in the investigation. All dimensions are in inches.

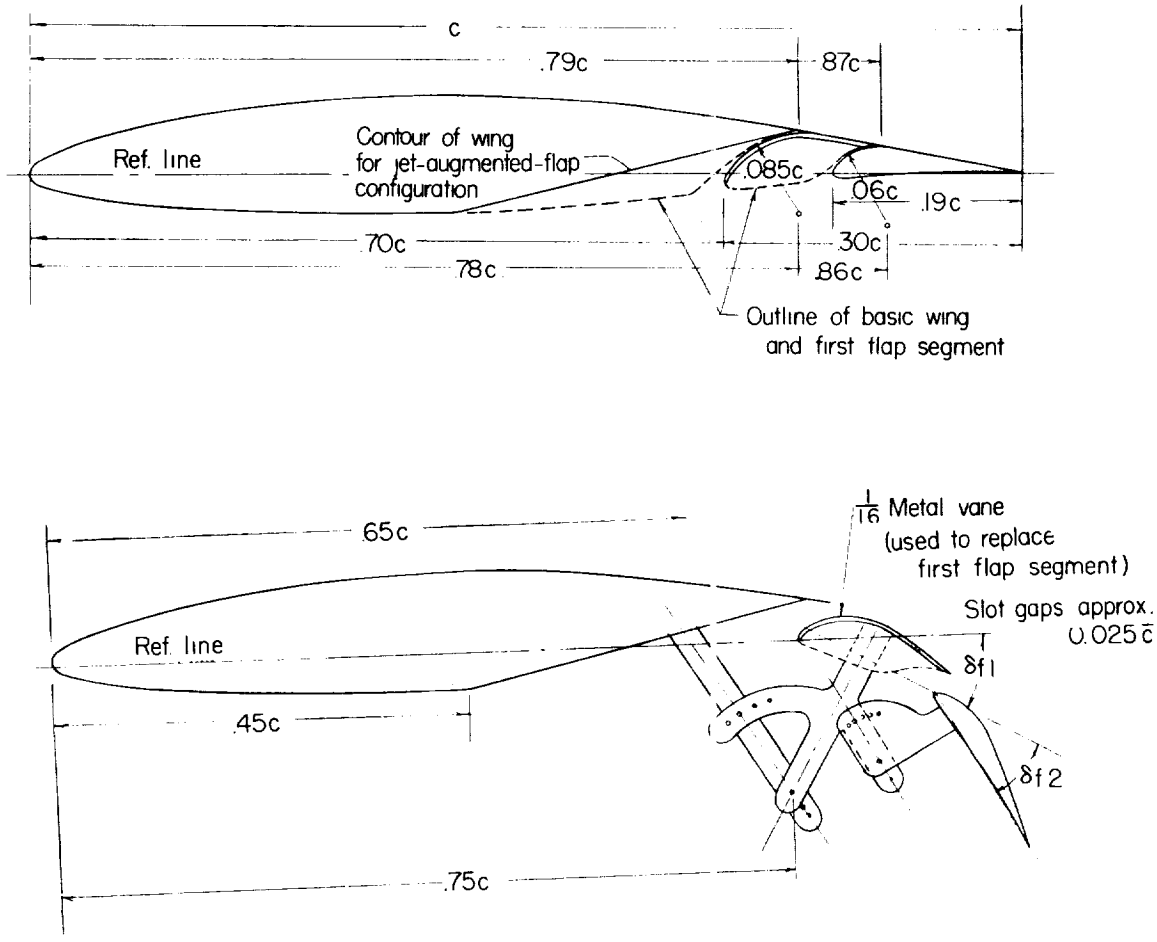

(b) Cross section of wing showing double slotted flap and flap mounting bracket.

Figure 3.- Concluded.

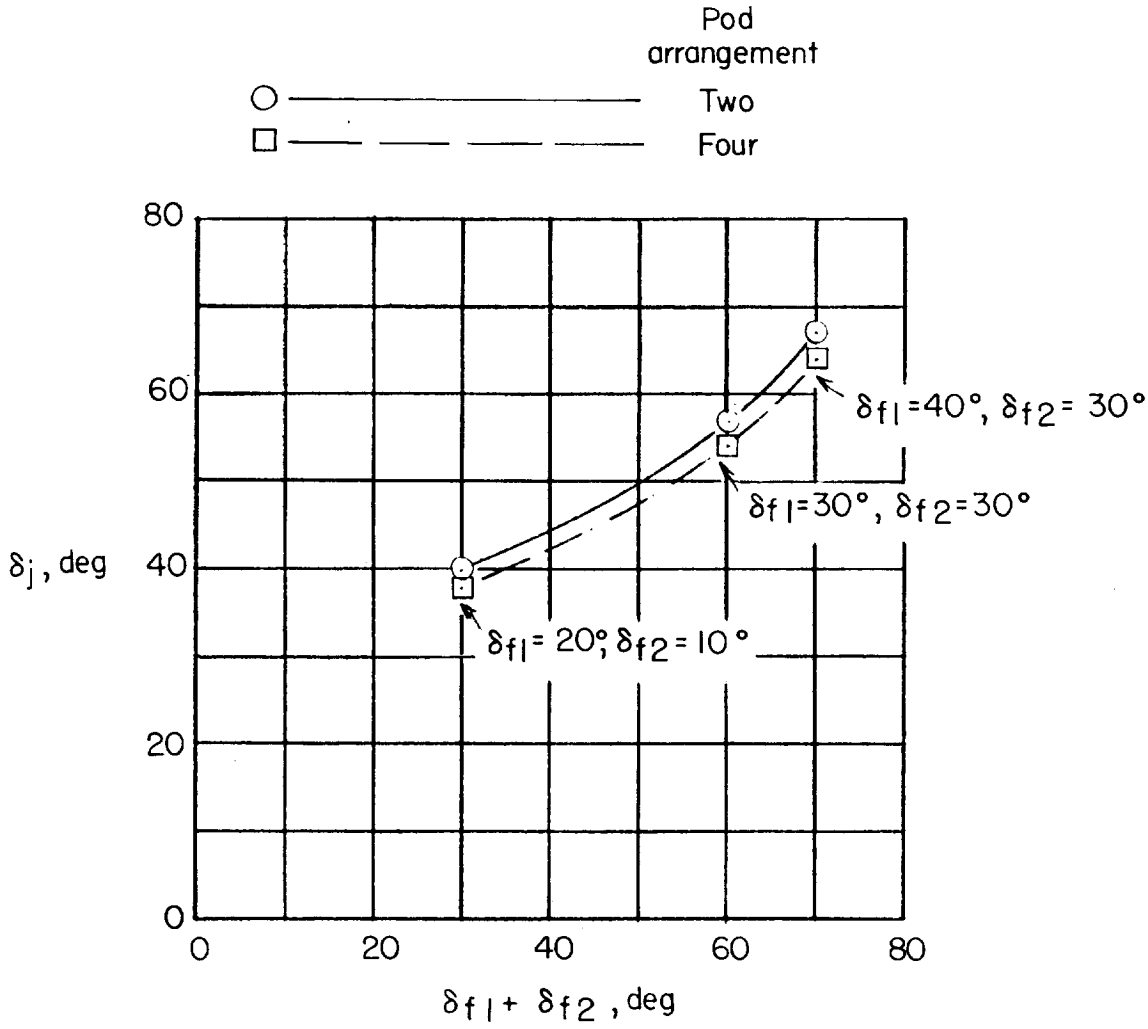

Figure 4.- Calibration of jet-deflection angles.

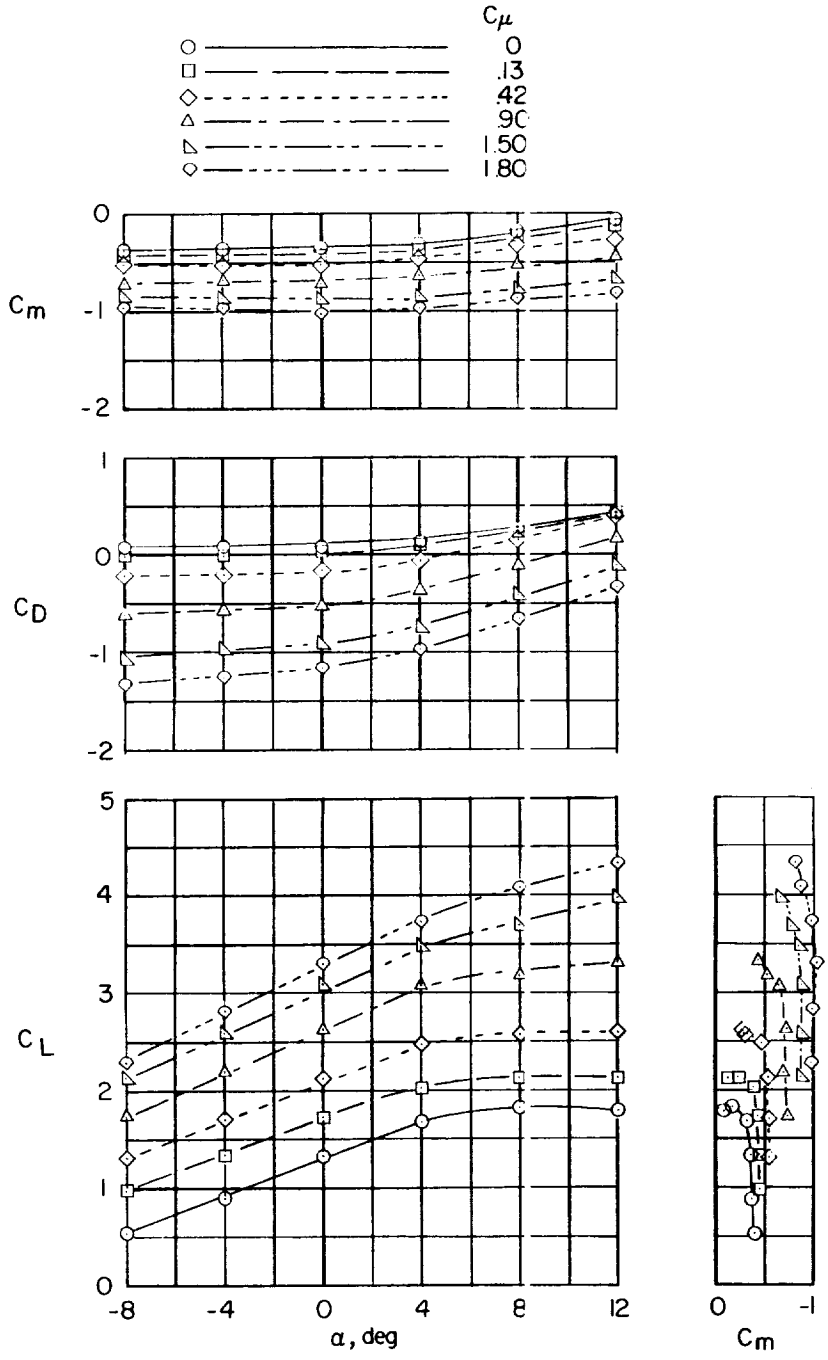

(a) Wing-fuselage combination.

Figure 5.- Longitudinal stability and trim characteristics of the model. Two-pod arrangement; $\delta_j = 40^\circ$.

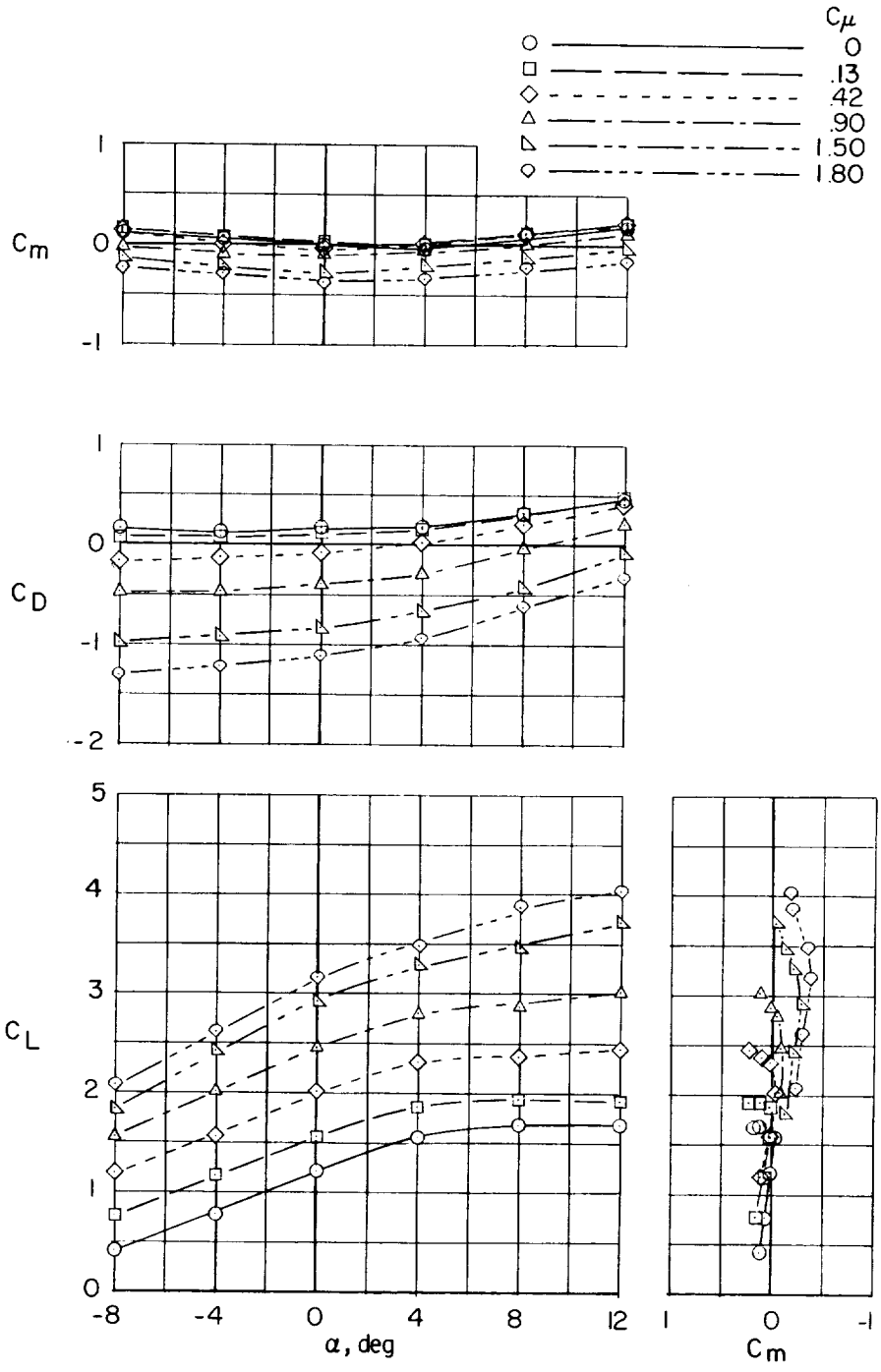

(b) $i_t = 10^\circ$; $\delta_e = -50^\circ$.

Figure 5.- Concluded.

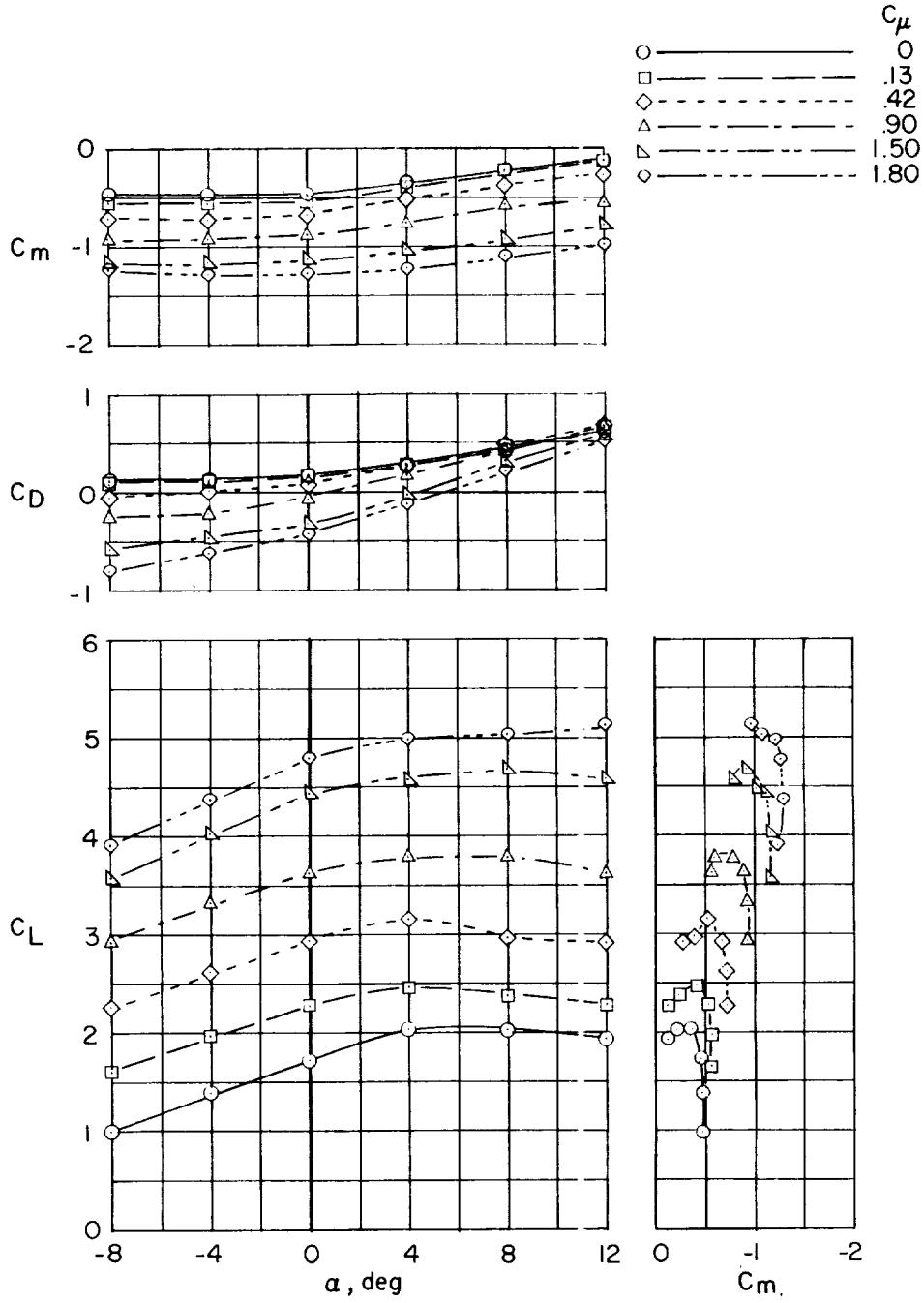

(a) Wing-fuselage combination.

Figure 6.- Longitudinal stability and trim characteristics of the model. Two-pod arrangement; $\delta_j = 57^\circ$.

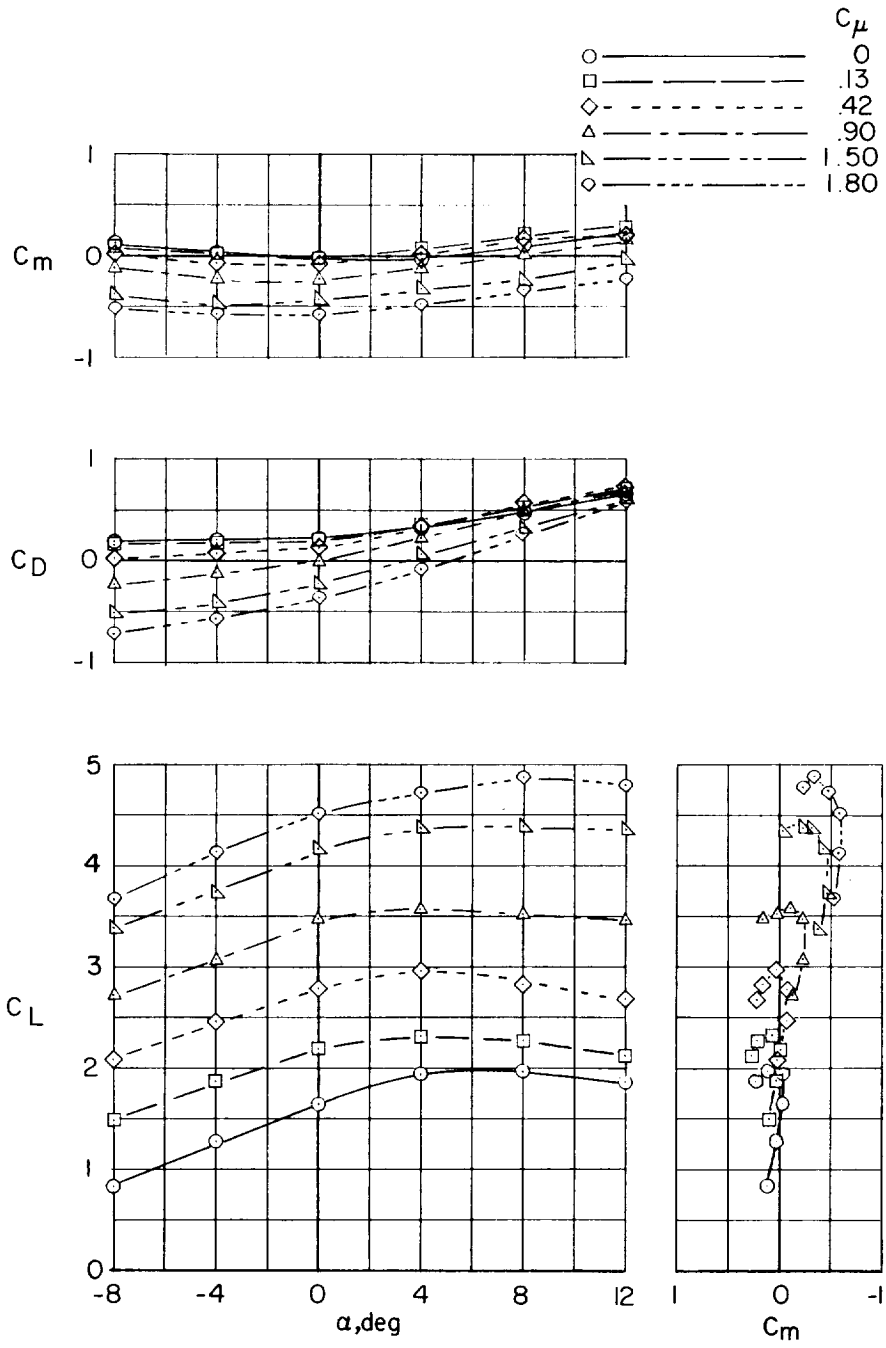

(b) $i_t = 10^\circ$; $\delta_e = -50^\circ$.

Figure 6.- Concluded.

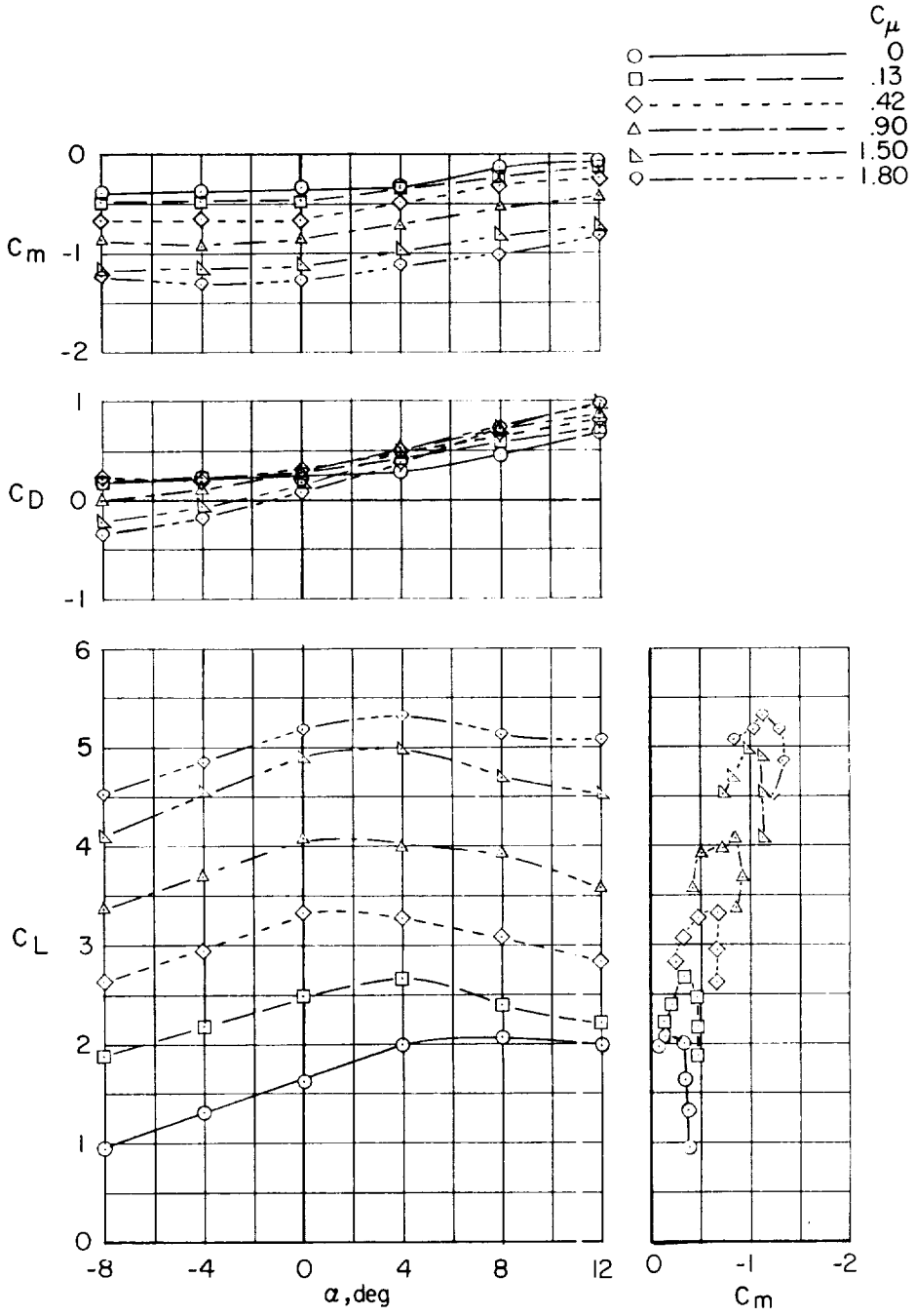

(a) Wing-fuselage combination.

Figure 7.- Longitudinal stability and trim characteristics of the model. Two-pod arrangement; $\delta_j = 67^\circ$.

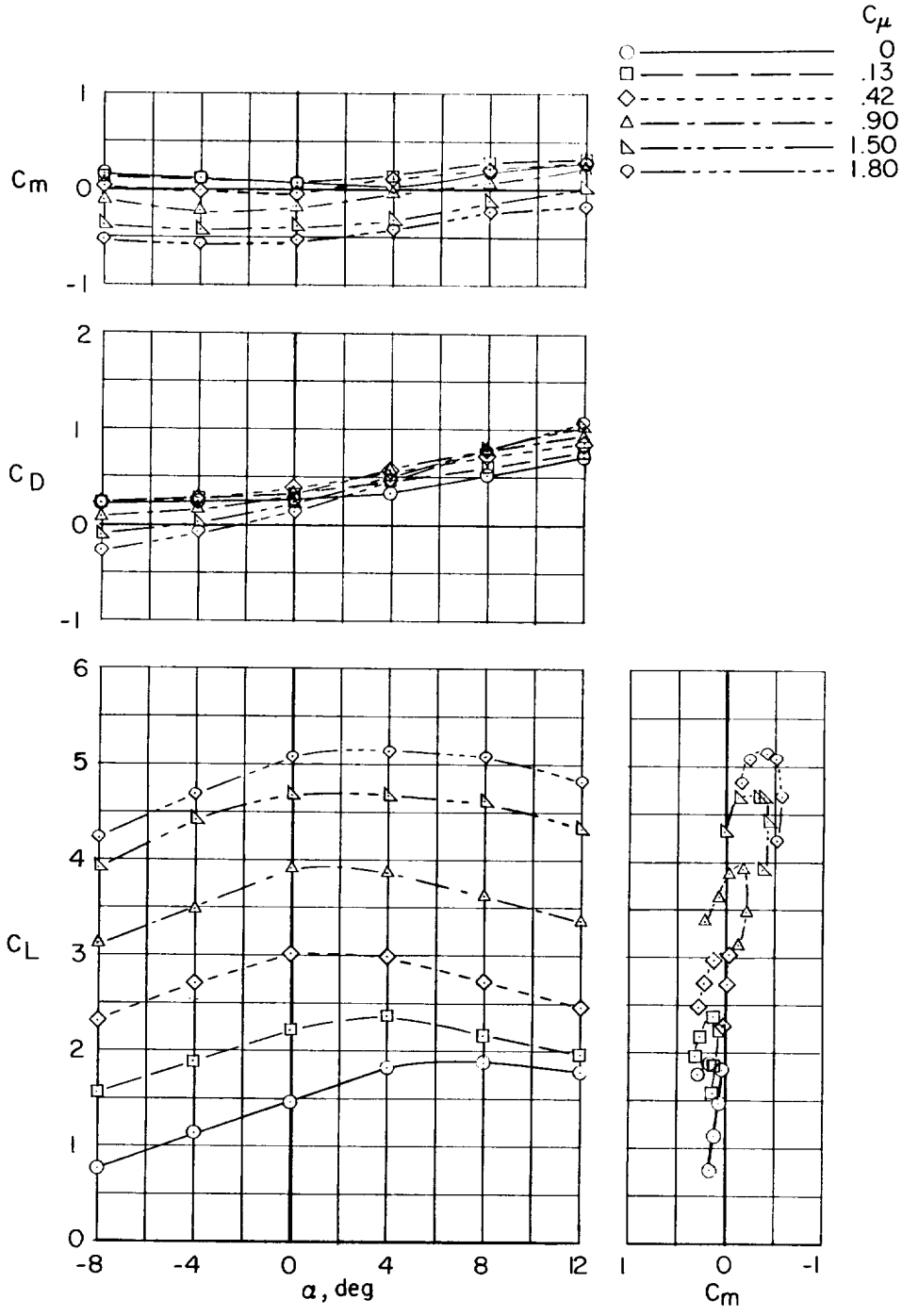

(b) $i_t = 10^\circ$; $\delta_e = -50^\circ$.

Figure 7.- Continued.

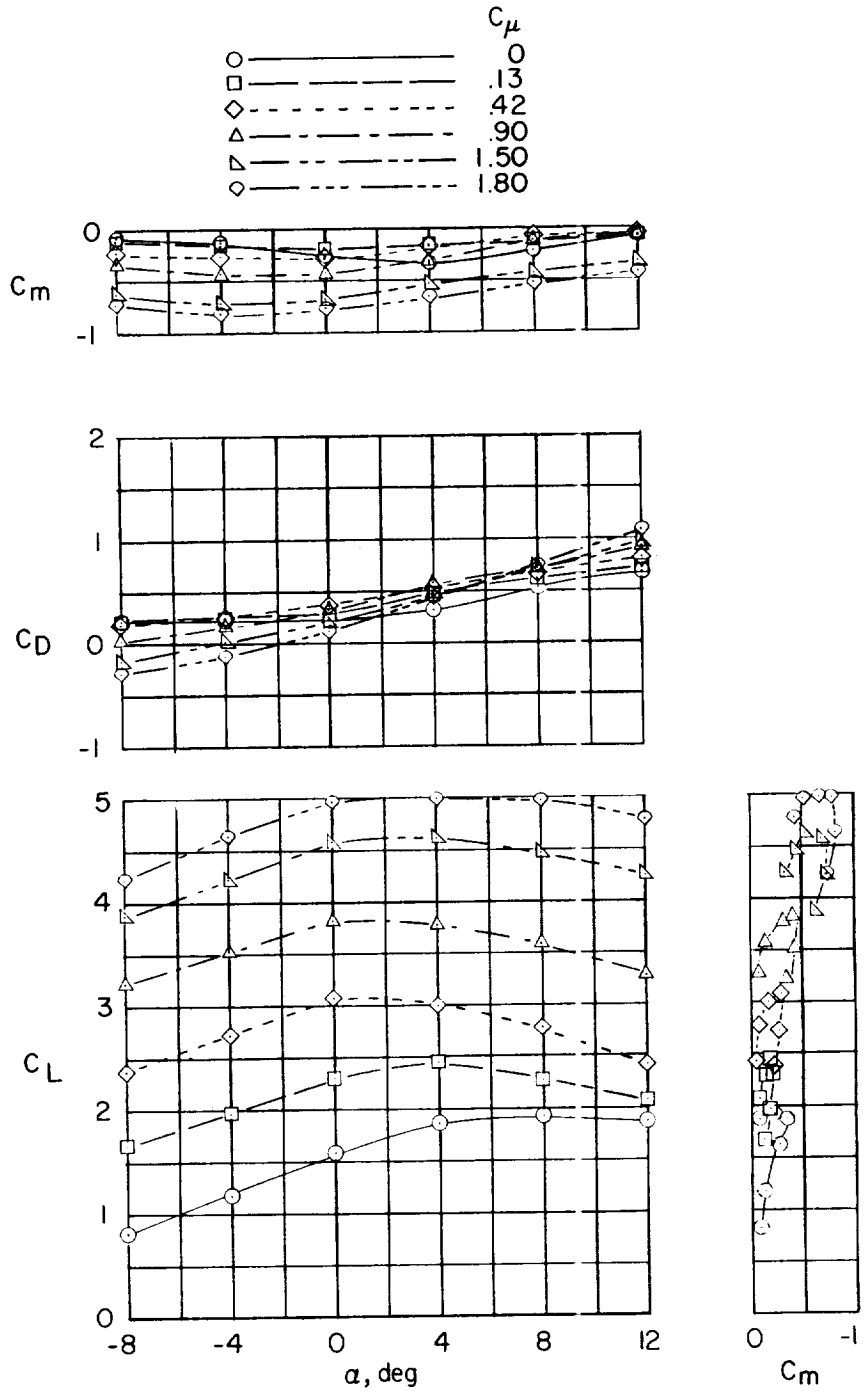

(c) $i_t = 20^\circ$; $\delta_e = -50^\circ$.

Figure 7.- Concluded.

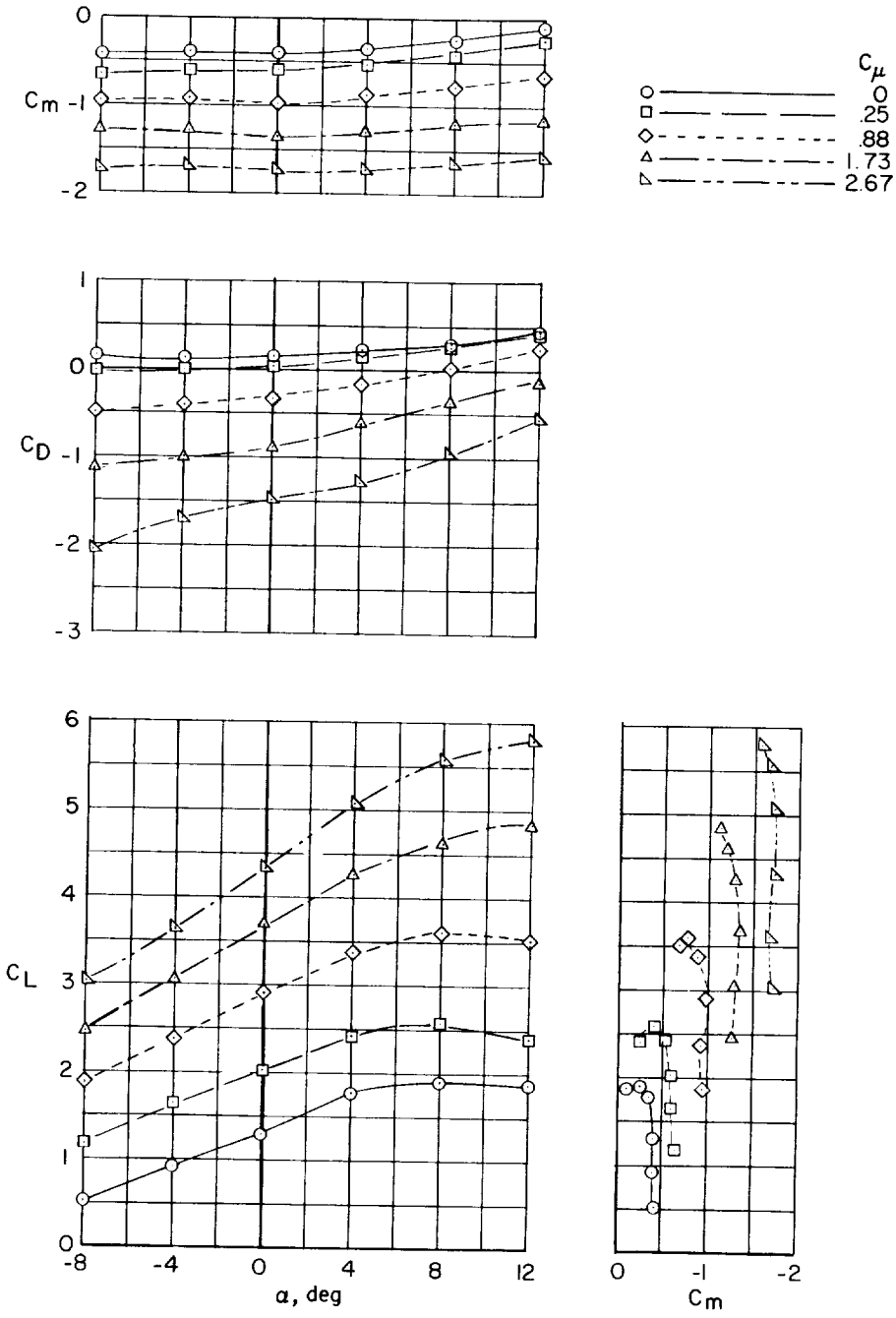

(a) Wing-fuselage combination.

Figure 8.- Longitudinal stability and trim characteristics of the model. Four-pod arrangement; $\delta_j = 36^\circ$.

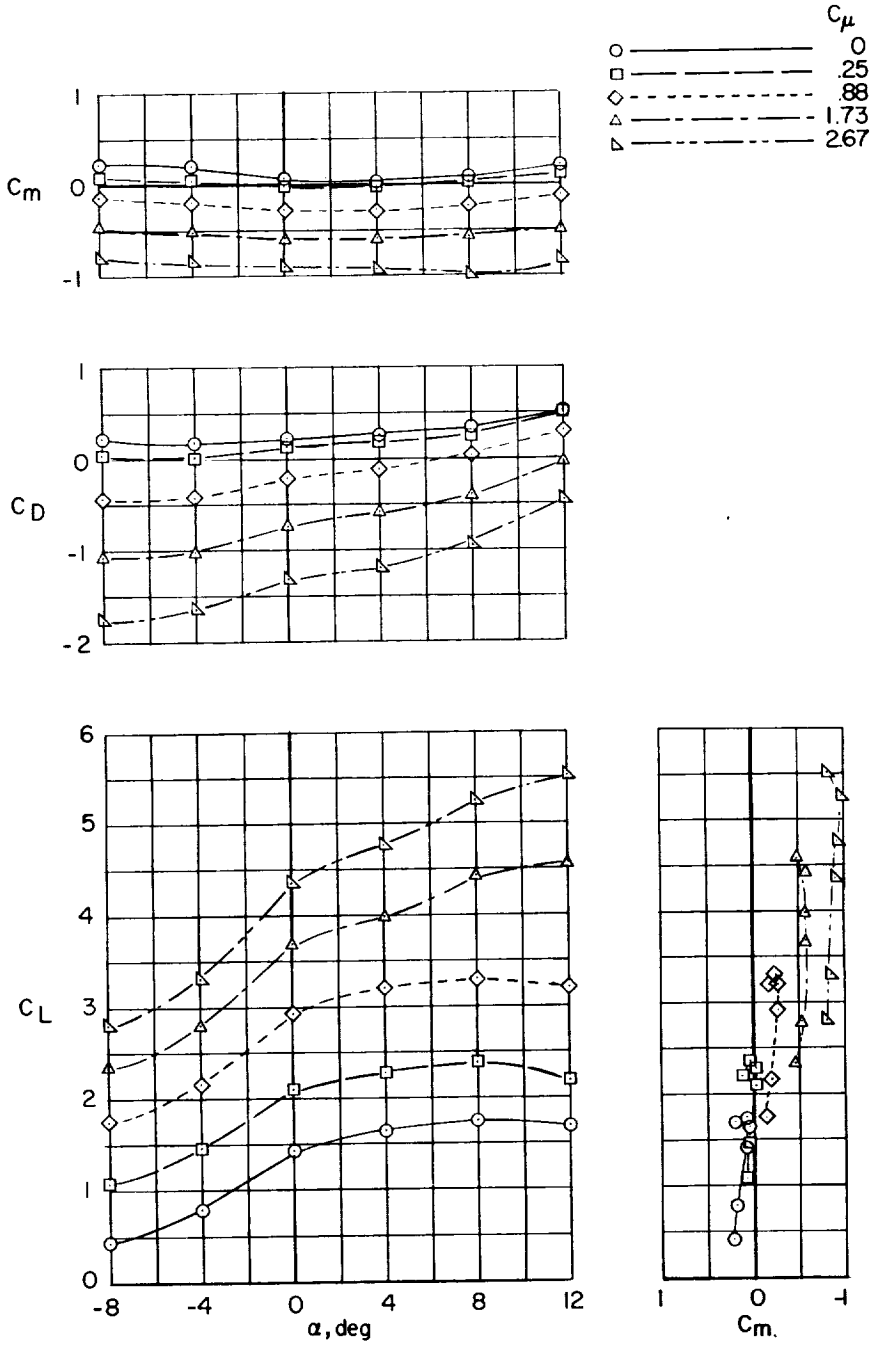

(b) $i_t = 10^o$; $\delta_e = -50^o$.

Figure 8.- Continued.

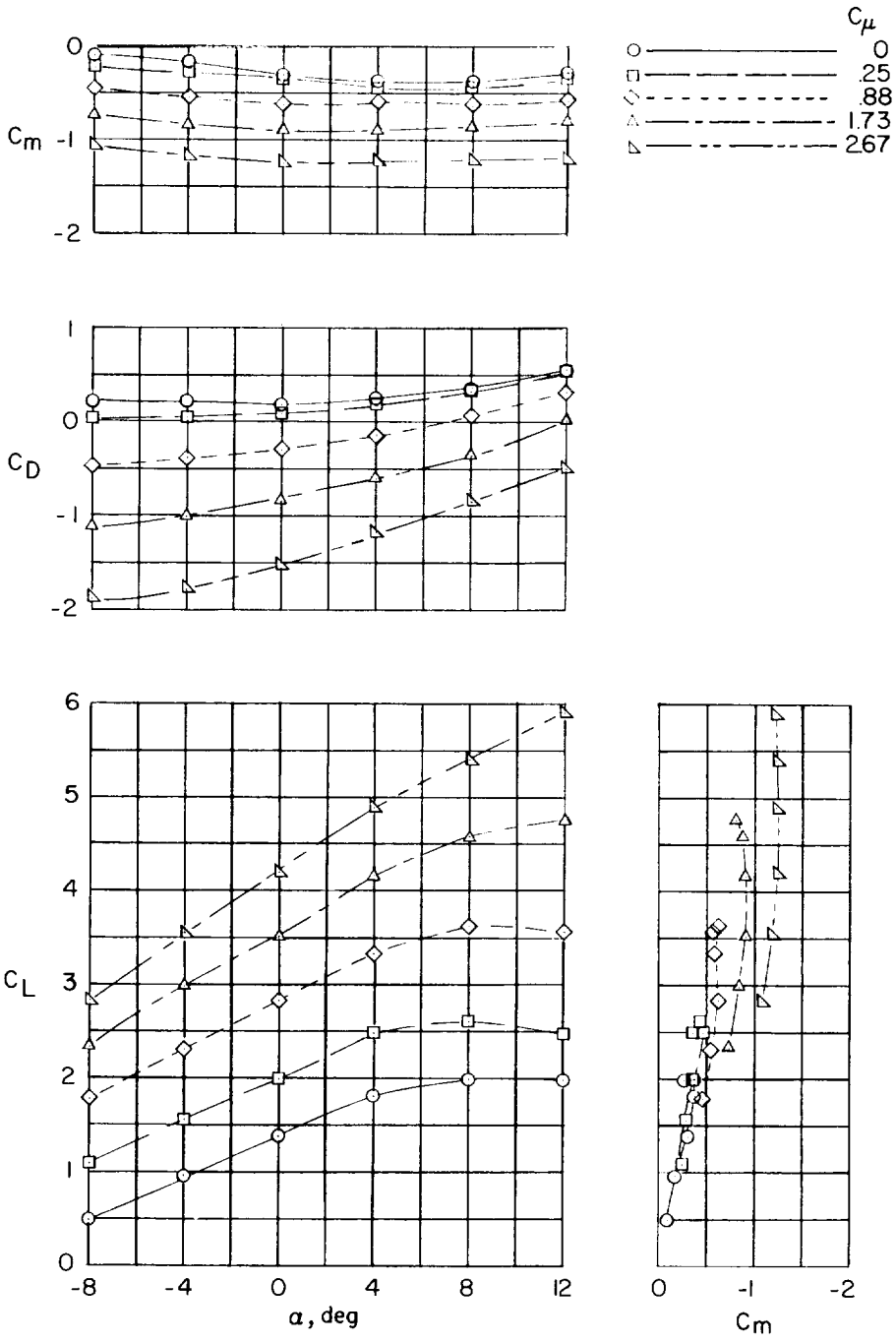

(c) $i_t = 20^\circ$; $\delta_e = -50^\circ$.

Figure 8.- Concluded.

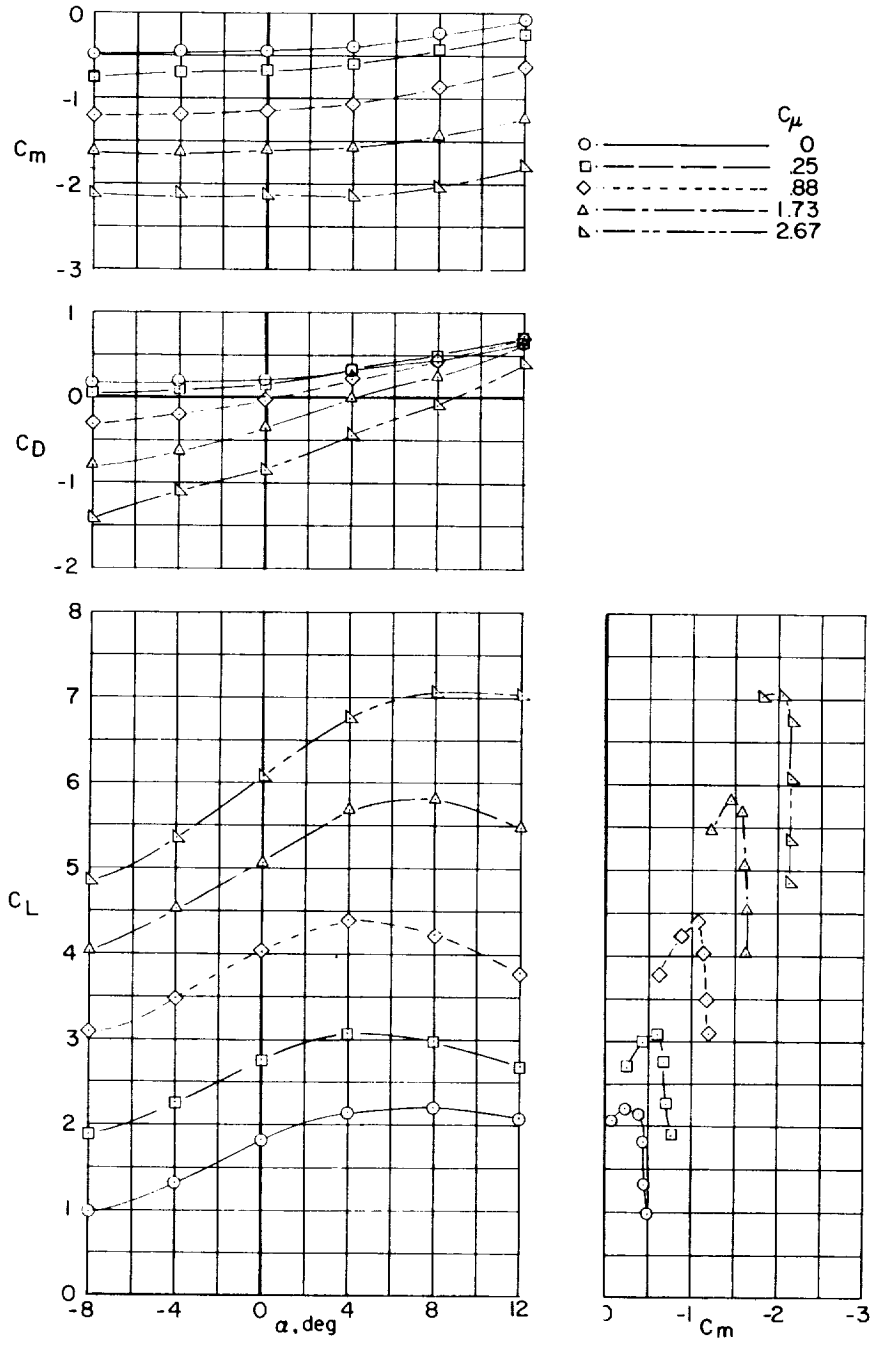

(a) Wing-fuselage combination.

Figure 9.- Longitudinal stability and trim characteristics of the model. Four-pod arrangement; $\delta_j = 54^\circ$.

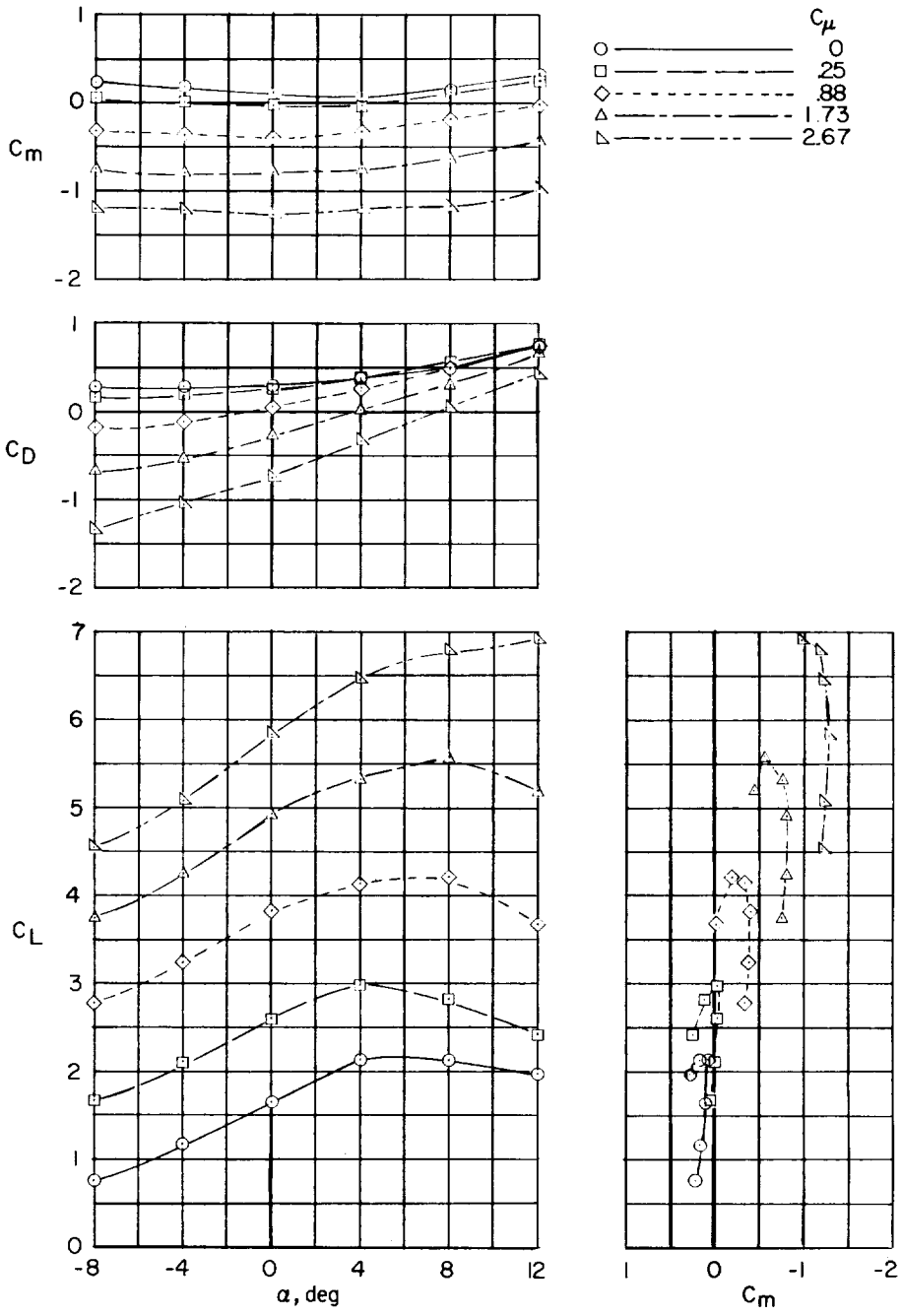

(b) $i_t = 10^\circ$; $\delta_e = -50^\circ$.

Figure 9.- Continued.

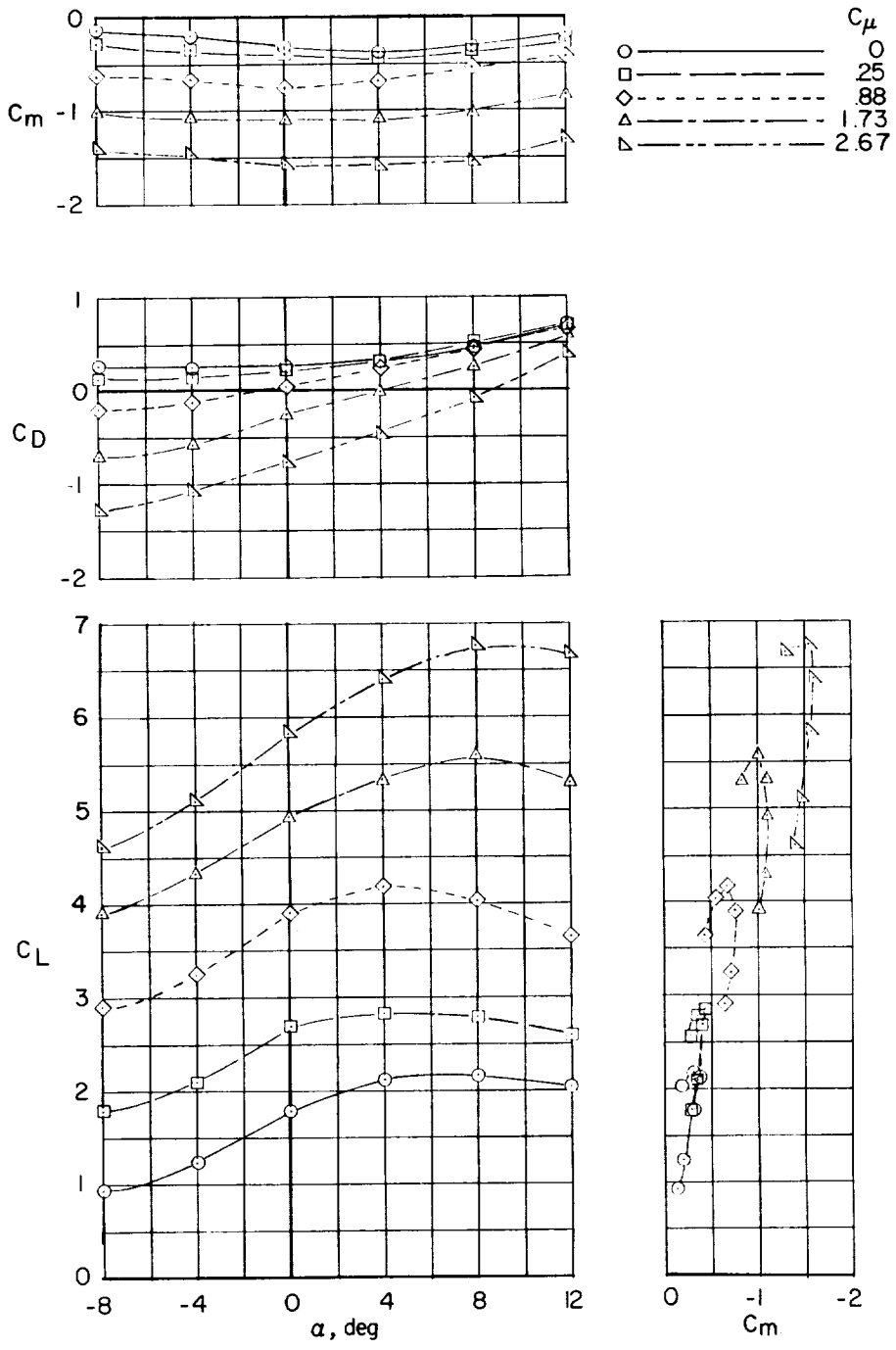

(c) $i_t = 20^\circ$; $\delta_e = -50^\circ$.

Figure 9.- Concluded.

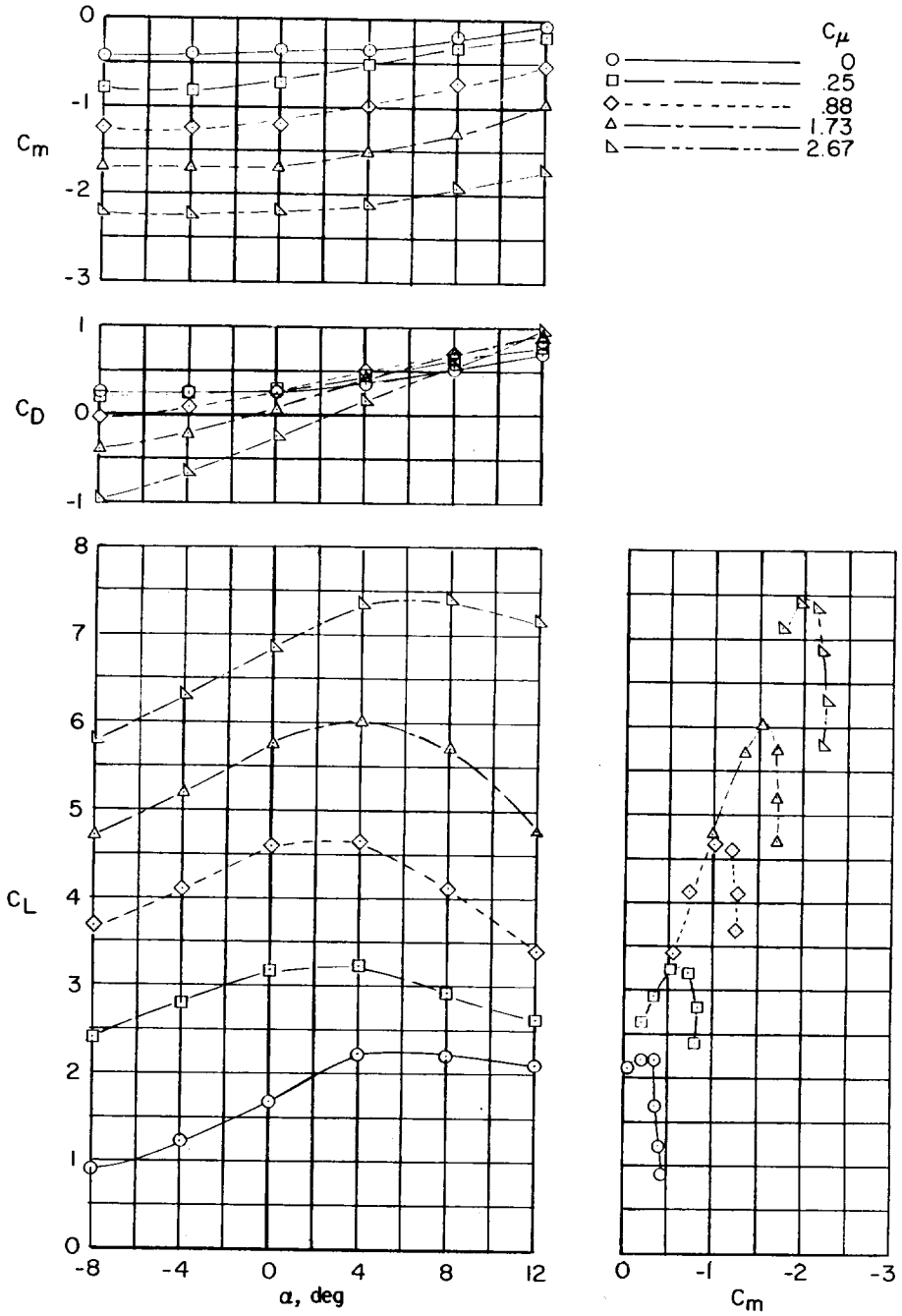

(a) Wing-fuselage combination.

Figure 10.- Longitudinal stability and trim characteristics of the model. Four-pod arrangement; $\delta_j = 64^\circ$.

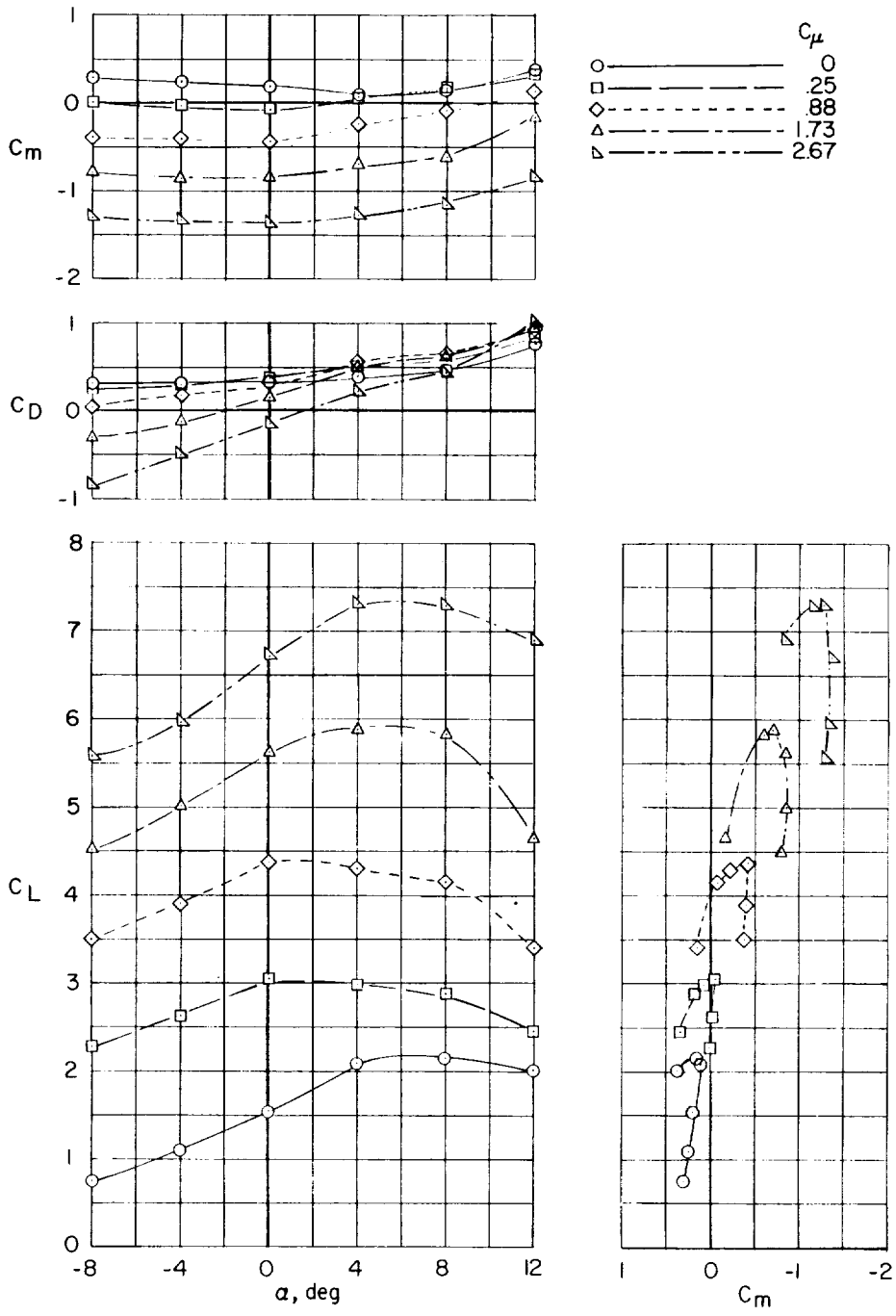

(b) $i_t = 10^\circ$; $\delta_e = -30^\circ$.

Figure 10.- Continued.

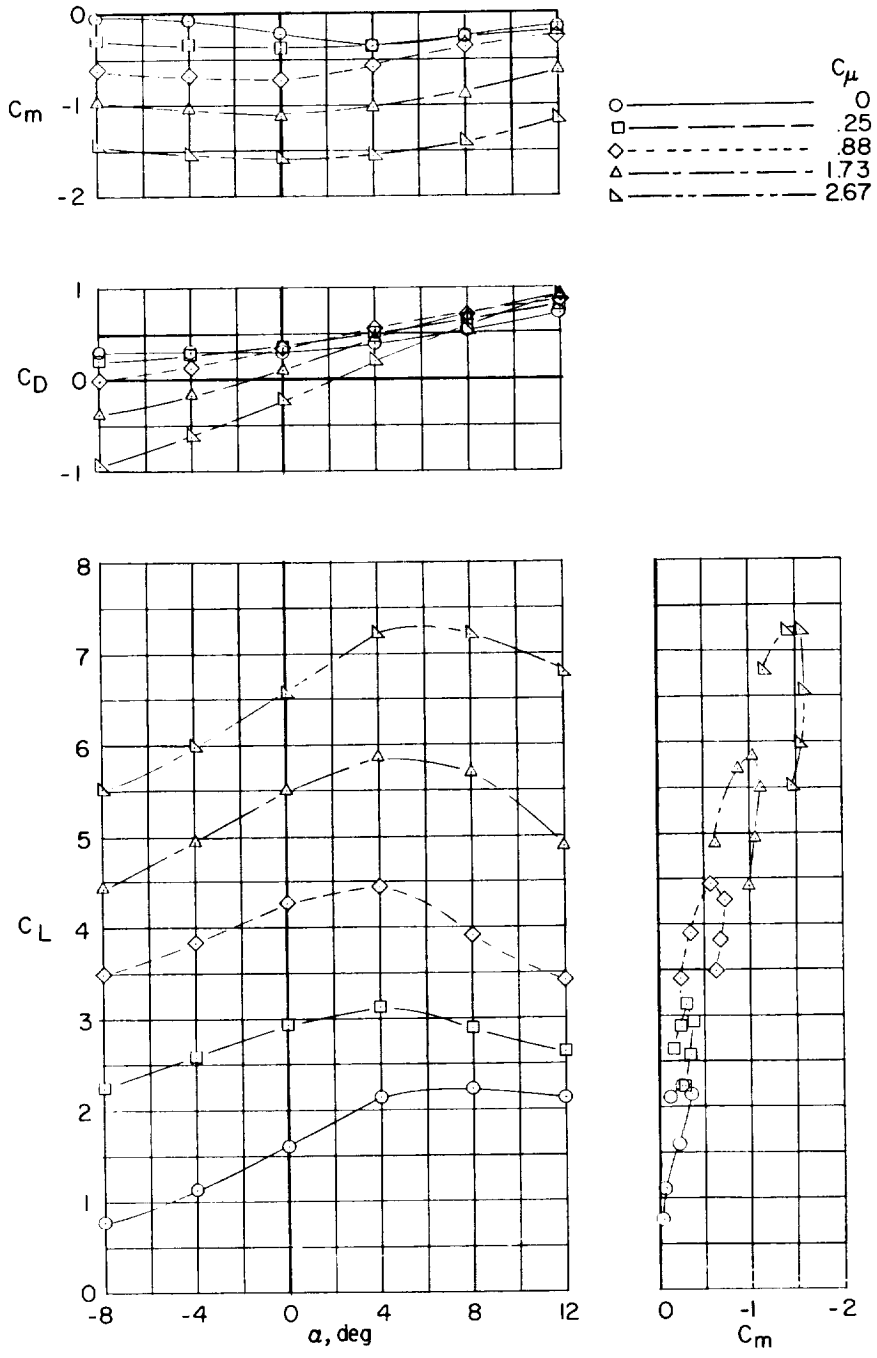

(c) $i_t = 20^\circ$; $\delta_e = -50^\circ$.

Figure 10.- Concluded.

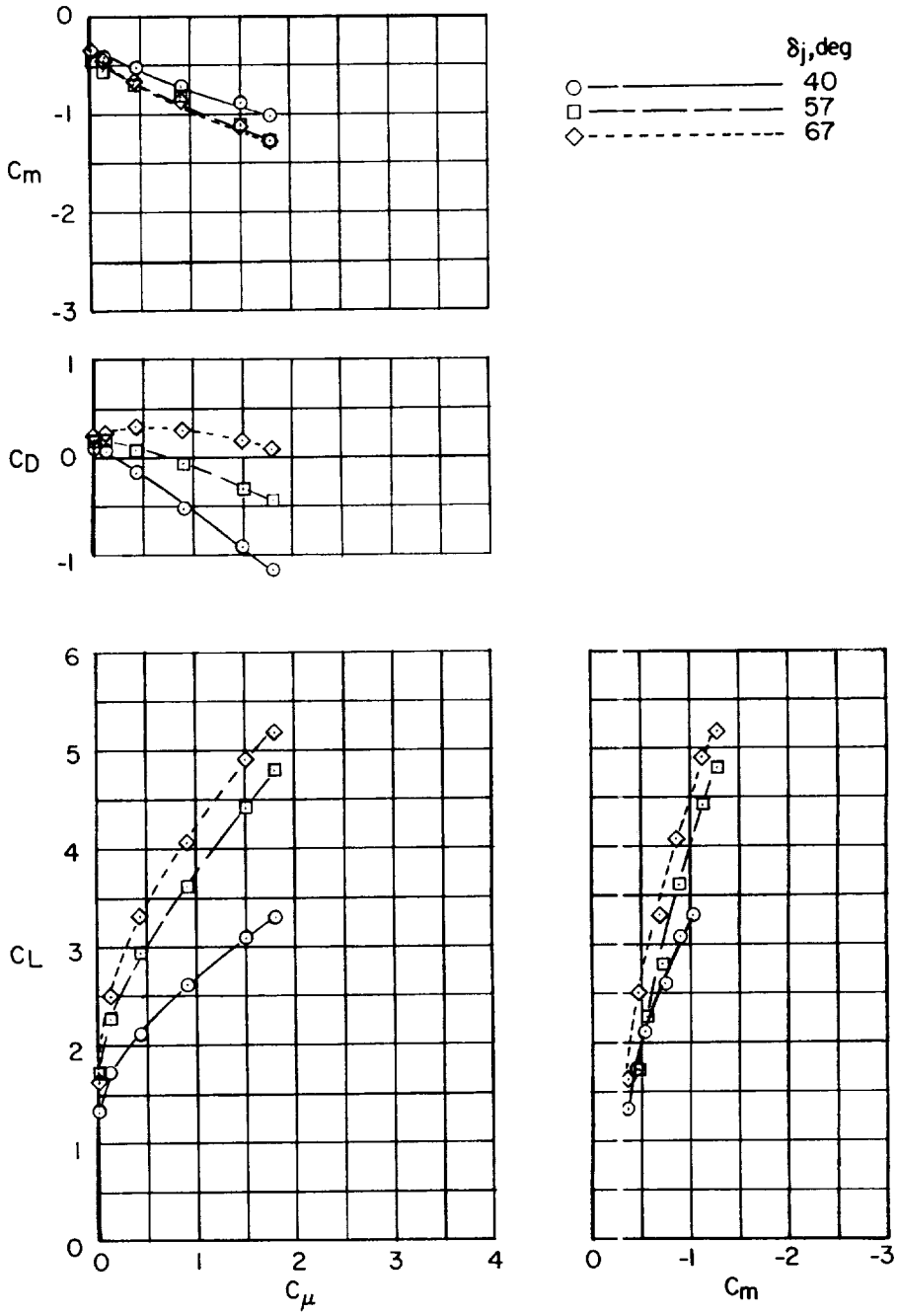

(a) Two-pod arrangement.

Figure 11.- Aerodynamic characteristics of the model. Horizontal tail off; $\alpha = 0^{o}$.

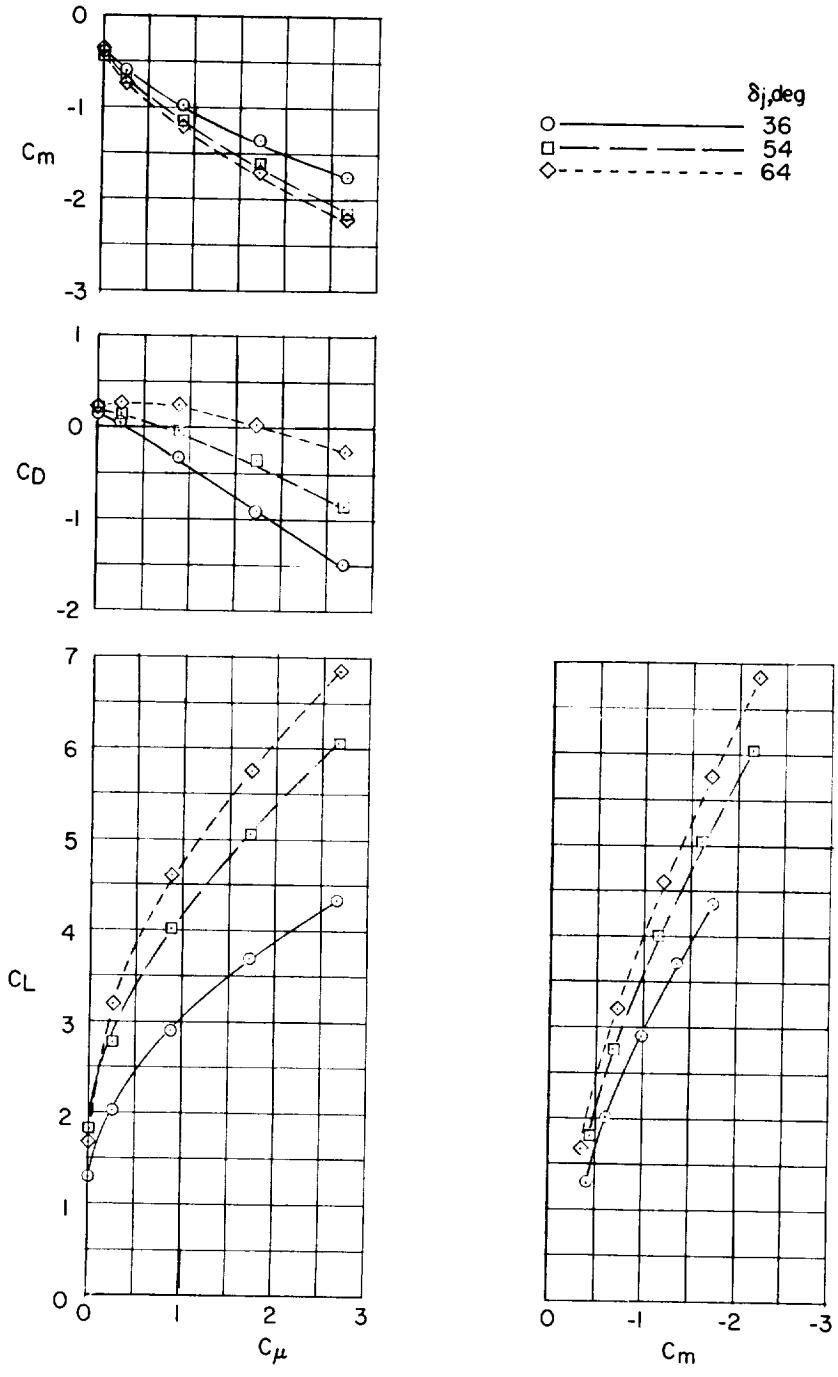

(b) Four-pod arrangement.

Figure 11.- Concluded.

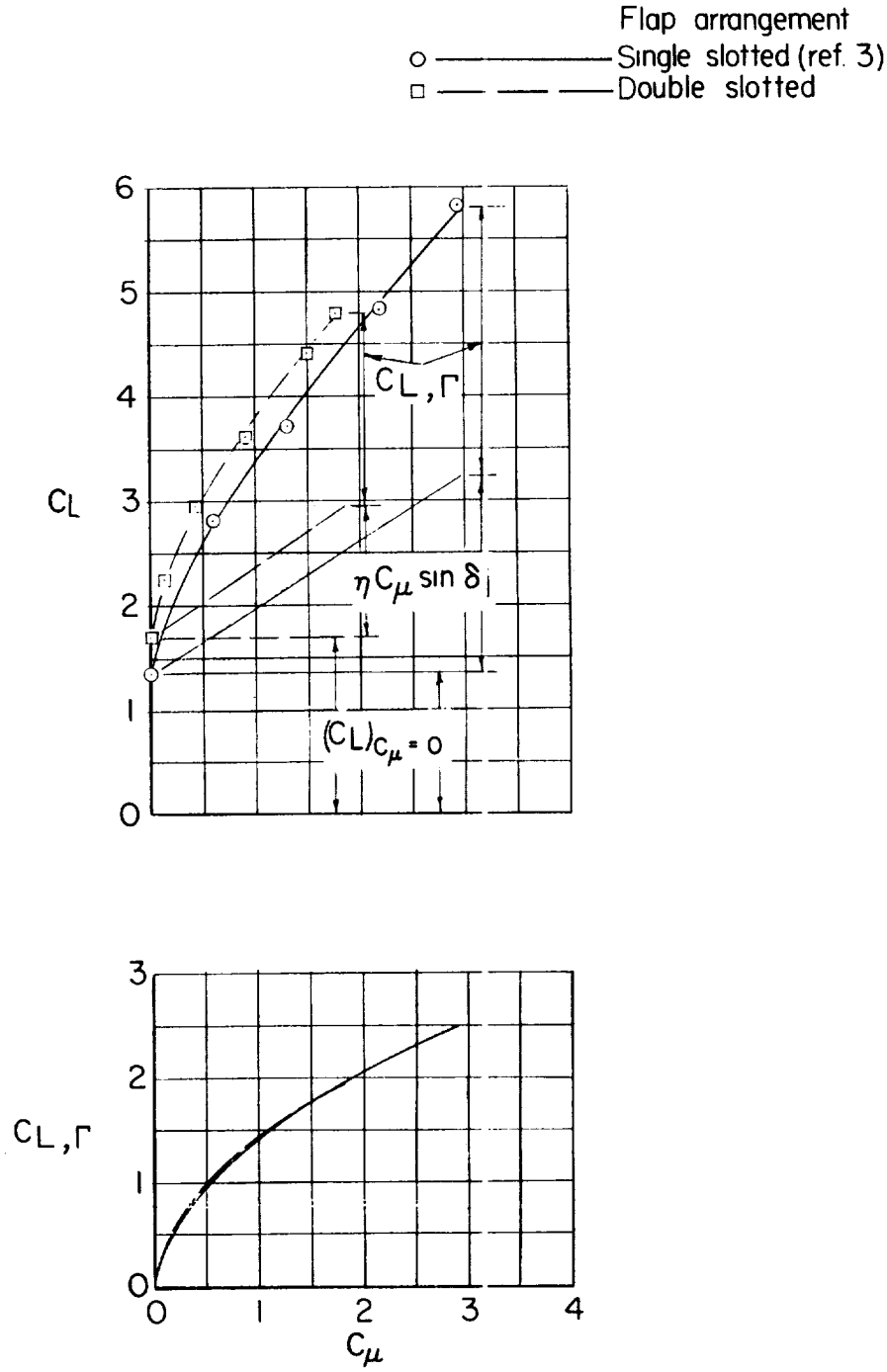

Figure 12.- Comparison of lift characteristics of the external-flow jet-augmented single- and double-slotted-flap arrangements. Two-pod arrangement; wing-fuselage combination; $\alpha = 0^\circ$; $\delta_j = 57^\circ$.

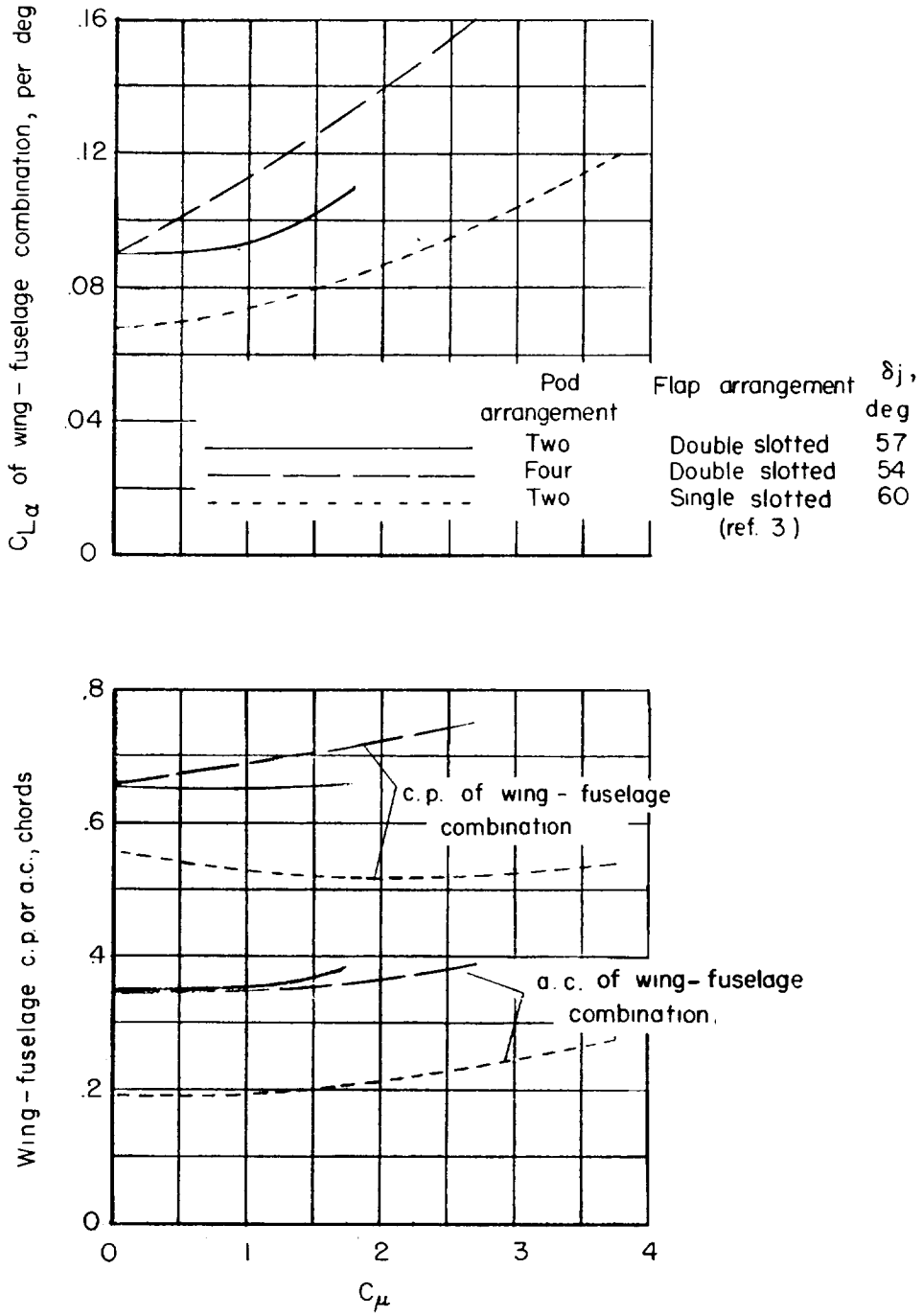

Figure 13.- Variation of center of pressure, lift-curve slope, and aerodynamic center of wing-fuselage combination with momentum coefficient. $\alpha = 0^o$.

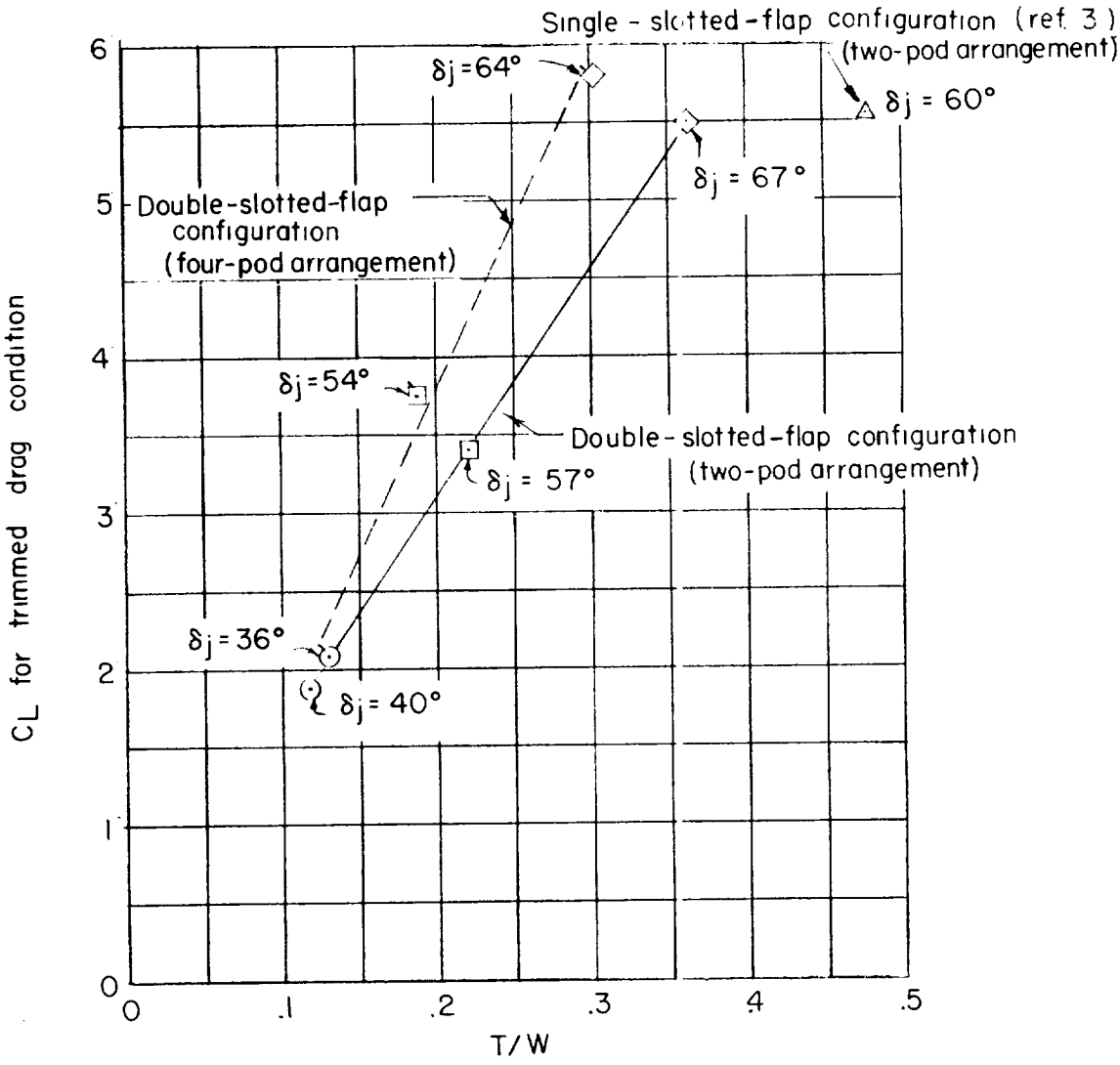

Figure 14.- Variation of C_L for trimmed drag condition with T/W. Wing-fuselage combination; $\alpha = 0^\circ$.

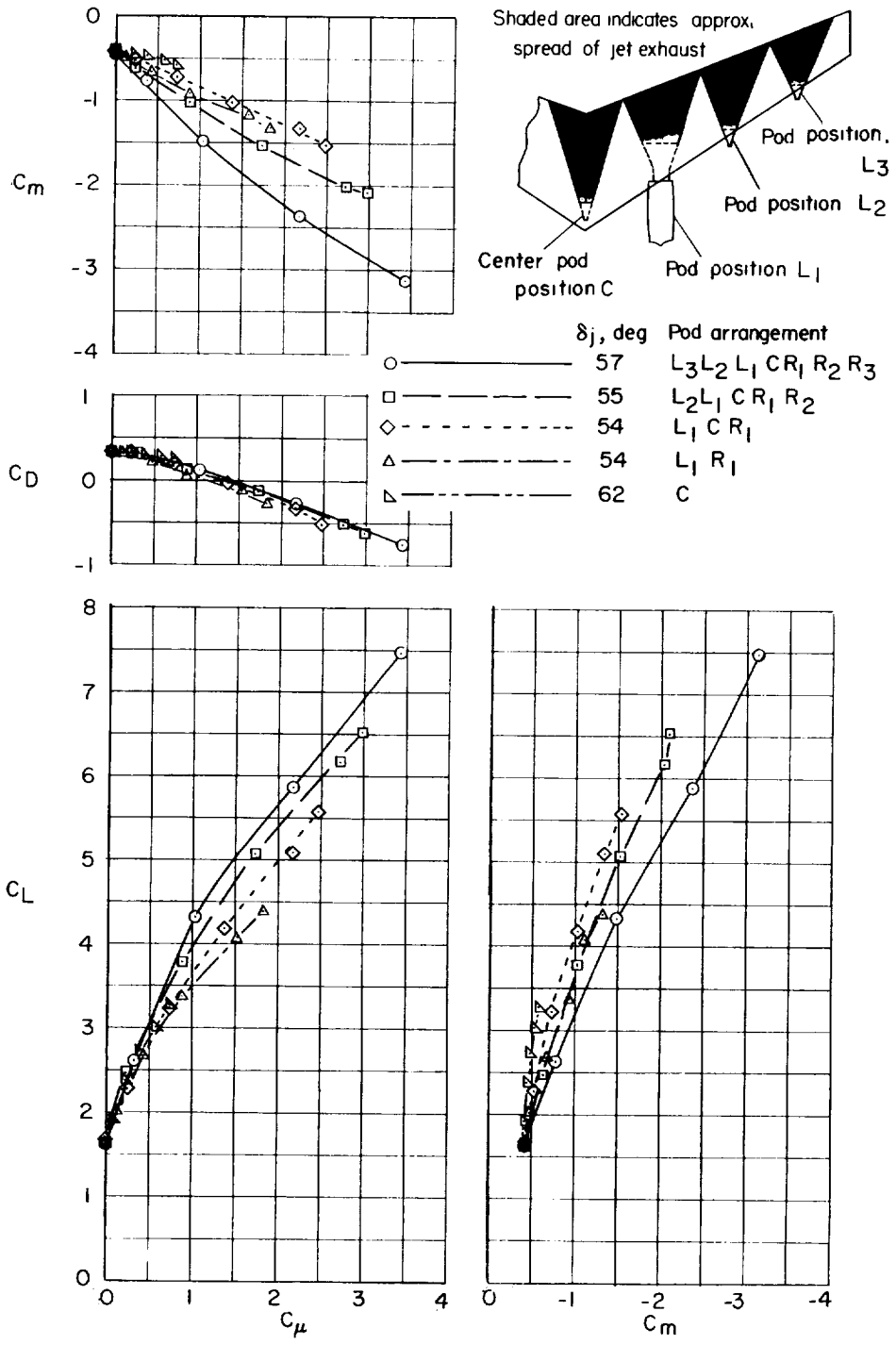

Figure 15.- Aerodynamic characteristics of the wing alone for several pod-mounted-engine arrangements. $\alpha = 0^{o}$.

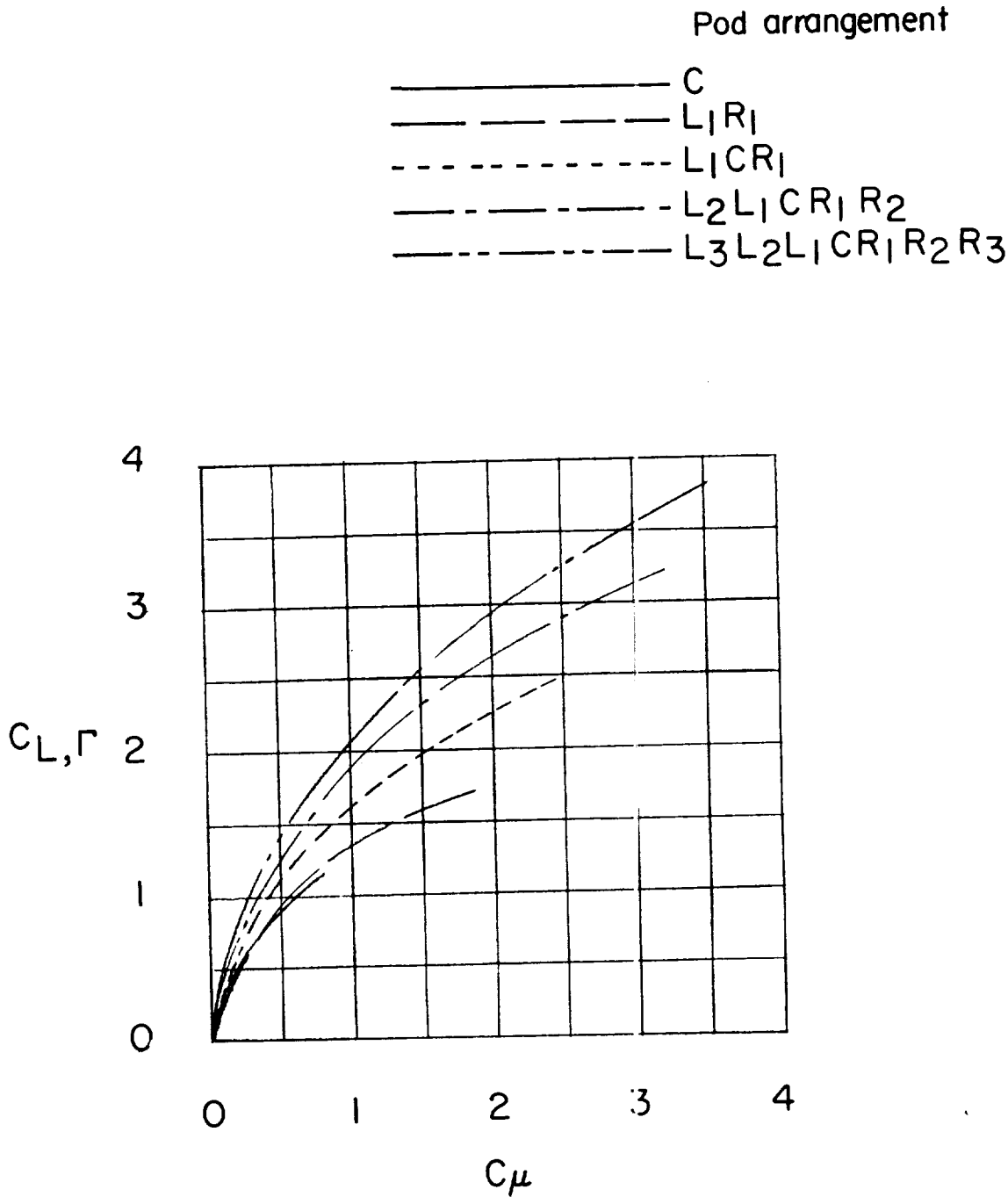

Figure 16.- Effect of varying the spanwise extent of blowing on the jet-circulation lift coefficient of the wing alone. $\delta_j = 60^\circ$; $\alpha = 0^\circ$.

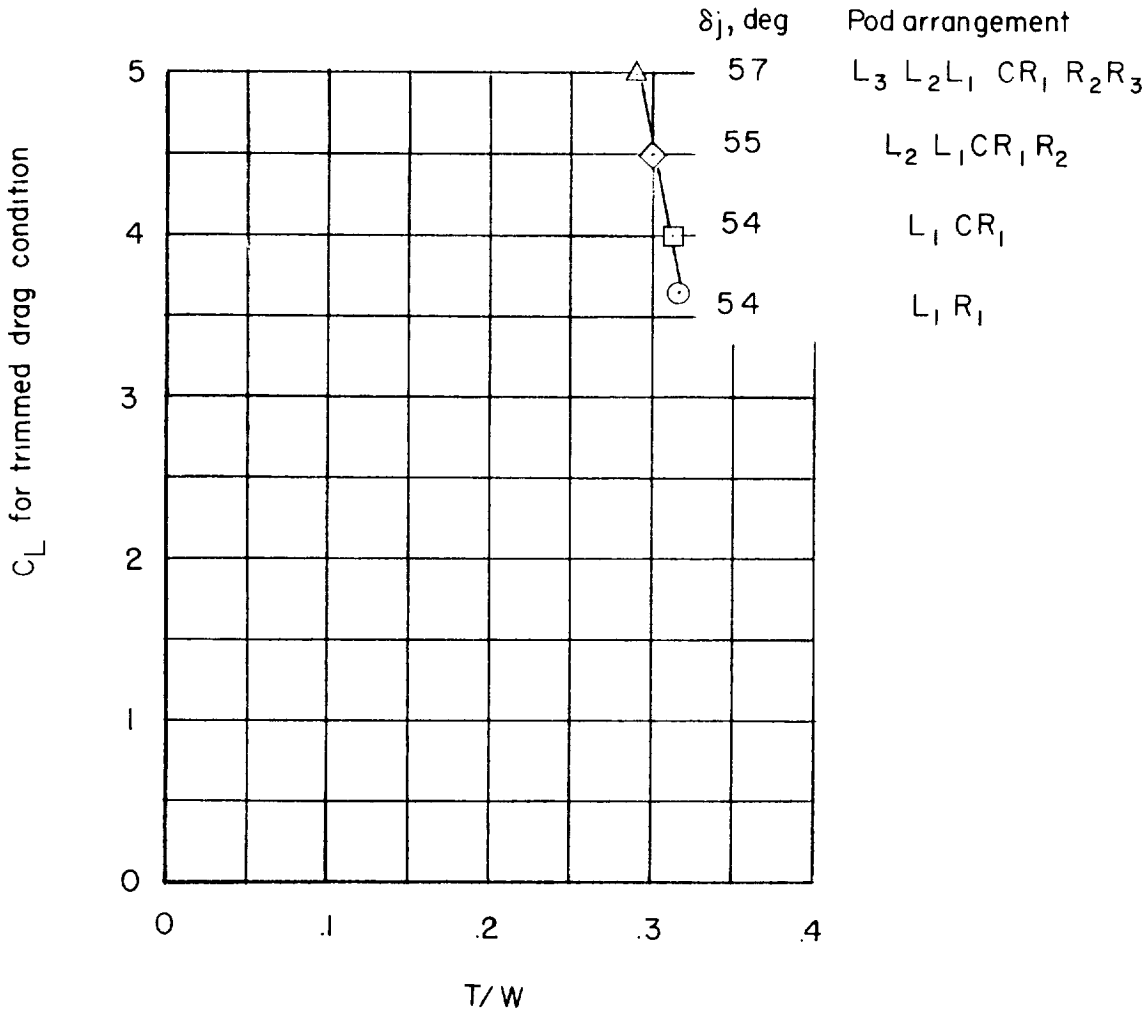

Figure 17.- Variation of C_L for trimmed drag condition with T/W.
Wing alone; $\alpha = 0^\circ$.

NASA - Langley Field, Va. L-164